International Journal of COPD

Dovepress
open access to scientific and medical research

Open Access Full Text Article

ORIGINAL RESEARCH

Systems pharmacology-based approach for dissecting the active ingredients and potential targets of the Chinese herbal Bufei Jianpi formula for the treatment of COPD

This article was published in the following Dove Press journal:
International Journal of COPD
7 December 2015
Number of times this article has been viewed

Peng Zhao[1,2]
Jiansheng Li[1,2]
Ya Li[1,2]
Yange Tian[1,2]
Yonghua Wang[2,3]
Chunli Zheng[3]

[1]Key Laboratory of Chinese Internal Medicine, Henan University of Traditional Chinese Medicine, [2]Key Laboratory of Chinese Internal Medicine, Collaborative Innovation Center for Respiratory Disease Diagnosis and Treatment and Chinese Medicine Development of Henan Province, Zhengzhou, [3]Center of Bioinformatics, College of Life Science, Northwest A&F University, Yangling, People's Republic of China

Background: The Chinese herbal Bufei Jianpi formula (BJF) provides an effective treatment option for chronic obstructive pulmonary disease (COPD). However, the systems-level mechanism underlying the clinical effects of BJF on COPD remains unknown.

Methods: In this study, a systems pharmacology model based on absorption filtering, network targeting, and systems analyses was applied specifically to clarify the active compounds and therapeutic mechanisms of BJF. Then, a rat model of cigarette smoke- and bacterial infection-induced COPD was used to investigate the therapeutic mechanisms of BJF on COPD and its comorbidity.

Results: The pharmacological system successfully identified 145 bioactive ingredients from BJF and revealed 175 potential targets. There was a significant target overlap between the herbal constituents of BJF. These results suggested that each herb of BJF connected with similar multitargets, indicating potential synergistic effects among them. The integrated target–disease network showed that BJF probably was efficient for the treatment of not only respiratory tract diseases but also other diseases, such as nervous system and cardiovascular diseases. The possible mechanisms of action of BJF were related to activation of inflammatory response, immune responses, and matrix metalloproteinases, among others. Furthermore, we demonstrated that BJF treatment could effectively prevent COPD and its comorbidities, such as ventricular hypertrophy, by inhibition of inflammatory cytokine production, matrix metalloproteinases expression, and other cytokine production in vivo.

Conclusion: This study using the systems pharmacology method, in combination with in vivo experiments, helped us successfully dissect the molecular mechanism of BJF for the treatment of COPD and predict the potential targets of the multicomponent BJF, which provides a new approach to illustrate the synergetic mechanism of the complex prescription and discover more effective drugs against COPD.

Keywords: chronic obstructive pulmonary disease, Bufei Jianpi formula, systems pharmacology

Introduction

Chronic obstructive pulmonary disease (COPD) is a serious health problem characterized primarily by irreversible airflow limitation due to an enhanced chronic inflammatory response in the airways and lung to noxious particles or gases.[1,2] Cigarette smoking is considered to be the major risk factor for COPD. Apart from smoking, bacterial infections accentuate airway inflammation, which accelerates irreversible disease progression.[3,4] To prevent the progression of COPD, millions of patients are

Correspondence: Jiansheng Li
Key Laboratory of Chinese Internal Medicine, Henan University of Traditional Chinese Medicine, 1 Jinshui Road, Zhengzhou 450046, People's Republic of China
Email li_js8@163.com

treated by drug therapies that include bronchodilators, steroids, and phosphodiesterase inhibitors. These drugs offer therapeutic benefit but cause serious side effects and cannot effectively reduce the progression and mortality of this disease. For instance, aminophylline is used as a bronchodilator in COPD. The commonest side effects are headache, nausea and vomiting, abdominal discomfort, and restlessness. Convulsions, cardiac arrhythmias, and death may occur at high concentrations.[5] Hence, there is a pressing need for the development of more effective therapies for COPD.[6–8]

Traditional Chinese medicine (TCM) is a comprehensive medicinal system that has provided effective relief of symptoms in COPD patients for thousands of years. Bufei Jianpi formula (BJF), a TCM, is composed of 12 medicinal herbs and has been proven effective for the treatment of COPD. Clinical studies revealed a variety of desirable pharmacological effects of BJF on COPD, such as alleviating the clinical symptoms of stable COPD patients, reducing the exacerbation frequency, delaying acute exacerbation, and improving pulmonary function and exercise capacity.[9] However, the molecular details regarding the effects of BJF on COPD are still unclear.

Studies on the pharmacological effects of TCM, such as BJF, face various difficulties for three main reasons. Firstly, identification of the complex active compounds contained in medicinal herbs is laborious and time-consuming. Secondly, there may be highly dynamic interactions among the active components, which also is one of the possible mechanisms of its treatment. Lastly, the multiple ingredients contained in most formulas and a lack of effective methods of study cause difficulties in identifying the targets of the herbal medicines.[10,11] Thus, a novel method that can identify the active compounds and the targets of herbal drugs, as well as clarify the mechanisms of action of Chinese medicine, is necessary.

Systems pharmacology, a new emerging research field of pharmacology, has provided promising avenues to help clarify the active compounds and therapeutic mechanisms of Chinese medicine.[11–14] This technological platform combines pharmacokinetics evaluation and drug–target–disease network analysis to get a global view of the multiple effects and mechanisms of Chinese herbal medicine.[15,16] Furthermore, the term "systems pharmacology" presently describes another promising new field of study that incorporates computational and experimental methods to explain the effects and molecular mechanisms of herbal medicines. In this work, we constructed a systems pharmacological model by integrating oral bioavailability predictions, target predictions, and network analysis to provide novel insights into the effect and mechanism of BJF. Finally, in order to supply the in vivo experimental evidence to validate the mechanisms of BJF action that were predicted in the computational experiment (systems pharmacology), we administered BJF to COPD model rats and examined the effect of BJF on cigarette smoke- and bacterial infection-induced pulmonary inflammatory responses, protease–antiprotease imbalance, and respiratory dysfunction.

Materials and methods

This trial was registered at the Chinese Clinical Trial Register Center: ChiCTR-TRC-11001406.

Chemicals and animals

Aminophylline was obtained from Shandong Xinhua Pharmaceutical Co., Ltd. (Zibo, People's Republic of China). *Klebsiella pneumoniae* (strain ID: 46114) was purchased from the National Center for Medical Culture Collection (Beijing, People's Republic of China). Antibodies against interleukin (IL)-6, IL-10, tumor necrosis factor (TNF)-α, soluble TNF-α receptor 2, collagen I, collagen III, collagen IV, endothelin (ET)-1, transforming growth factor (TGF)-β, vascular endothelial growth factor (VEGF), basic fibroblast growth factor (bFGF), matrix metalloproteinase (MMP)-2, MMP-9, and tissue inhibitor of MMP (TIMP)-1 were purchased from Santa Cruz Biotechnology, Inc. (Dallas, TX, USA). The RNeasy kit was obtained from Qiagen (Valencia, CA, USA). Mayer's hematoxylin and 1% eosin alcohol solution were purchased from MUTO Pure Chemicals (Tokyo, Japan). In all, 42 Sprague Dawley rats (21 male and 21 female; 200±20 g) were purchased from the Experimental Animal Center of Henan Province (Zhengzhou, People's Republic of China). The animals were housed in cages with free access to food and tap water under standard conditions of humidity (50%±10%), temperature (25°C±2°C), and light (12 hours light/12 hours dark cycle). All animals were handled with humane care throughout the experiment.

Dataset construction

All ingredients from the 12 herbs of BJF were collected mainly from the Chinese Academy of Sciences Chemistry Database (http://www.organchem.csdb.cn), Chinese Herbal Drug Database, and the literature.[17–20] For orally administered drugs, glucosides can be metabolized extensively to their deglycosylation products by enteric bacteria in the intestinal tract;[21] thus, both glucosides and deglycosylation products are considered to be the constituents of herbal drugs. Taken together, a total of 886 chemicals were included: 87 in

Astragali Radix (AR), 38 in Polygonati Rhizoma (PR), 134 in Codonopsis Radix (CR), 55 in Atractylodis Macrocephalae Rhizoma (AMR), 34 in Poria (Po), 17 in Fritillariae Thunbergii Bulbus (FTB), 139 in Magnoliae Officinalis Cortex (MOC), 63 in Citri Reticulatae Pericarpium (CRP), 91 in Asteris Tatarici Radix (ATR), 28 in Pheretima, 193 in Ardisiae Japonicae Herba (AJH), and 130 in Epimedii Herba (EH) (Table S1).

OB screening

Oral bioavailability (OB), which indicates the capability of the orally administered drug be delivered to systemic circulation, is one of the most important pharmacokinetic parameters in drug screening.[22,23] In this work, the OB values were predicted by a robust in silico model OBioavail 1.1.[23] Molecules with OB ≥30% were obtained as candidate compounds for further analysis. The threshold used in our work was selected primarily to: 1) extract as much information as possible from the BJF components with the least number of compounds and 2) explain the obtained model scientifically using the reported pharmacological data.

Drug-likeness prediction

The drug-likeness index was used to evaluate the structural similarity between the herbal ingredients and the drugs in the DrugBank database (http://www.drugbank.ca/) and help remove compounds that are considered to be chemically and pharmacologically unsuitable as drugs.[24] In this study, the database-dependent drug-likeness prediction approach was calculated as follows:

$$T(A,B) = \frac{A \cdot B}{\|A\|^2 + \|B\|^2 - A \cdot B} \quad (1)$$

where A represents the herbal compounds and B represents the average molecular drug-likeness index of all compounds in the DrugBank database. A drug-likeness index ≥0.18 (average value for all DrugBank molecules) was set as the threshold to select drug-like compounds. The compounds that overcame both the OB and drug-likeness screens were retained as candidate compounds. In addition, several compounds such as tangshenoside II, atractylenolide I, atractylenolide III, ergosterol, naringin, hesperidin, bergenin, icariside I, and anhydroicaritin initially were omitted according to these screening rules; however, these compounds were supported by literature evidence and, therefore, also were obtained as candidate compounds for further analysis.[21–29]

Drug targeting analysis

The targets related to the candidate compounds were predicted by the systematic drug targeting tool,[30] which efficiently integrates the chemical, genomic, and pharmacological information for drug targeting by RandomForest and Support Vector Machine methods. This model shows a good predictive performance for drug–target interactions, and the results are represented by a probability of interactions between each compound and a number of targets from the DrugBank database. In this work, the compound–target interactions with a Support Vector Machine score ≥0.8 and RandomForest score ≥0.7 were considered as potential targets of the candidate compounds. Then, the diseases related to the potential targets were collected from the Therapeutic Target, DrugBank, and PharmGkb databases, and the obtained diseases were classified further into different groups according to the MeSH Browser (2014 MeSH).

Network construction

The herbs, candidate compounds, potential targets, and diseases related with the potential targets were used to build the compound–target and target–disease networks. These networks were generated by Cytoscape 3.2.1.[31] In the graphical networks, nodes encode the herbs, compounds, target proteins, or diseases, and edges represent the herb–compound, herb–target, or target–disease interactions. The degree of a node is the number of edges associated with it. Nodes with a high degree can be considered the key nodes in a network. The topological properties of the networks were analyzed using the Network Analysis plugin of Cytoscape.[32]

COPD model and drug administration

Rats were placed into a chamber connected to a cigarette smoke-producing apparatus (volume 300 L) and exposed to the tobacco (Hongqi Canal® Filter tip cigarette; tobacco type, tar: 10 mg; nicotine content: 1.0 mg; carbon monoxide: 12 mg, Henan Tobacco Industry, Zhengzhou, People's Republic of China) smoke of eight cigarettes for 30 minutes, twice per day with 3-hour smoke-free intervals during the first 2 weeks. Then, COPD rats were exposed to the smoke of 15 cigarettes for 30 minutes, thrice per day with 3-hour smoke-free intervals from weeks 3 to 12. Additionally, 100 µL of *Klebsiella* pneumonia suspension (6×10^8 CFU/mL) was dropped slowly into the nasal cavities of smoke-exposed rats every 5 days from weeks 1 to 8. On week 9, two COPD rats were sacrificed to obtain the lung tissues to confirm that this rat model was successful.[33]

COPD rats were divided into three groups with 10 rats each (week 9). Then, COPD rats were intragastrically administrated normal saline (2 mL), BJF (4.84 g/kg), and aminophylline (2.3 mg/kg) every day for 12 weeks. The control rats also were administrated intragastrically normal saline (2 mL) every day for 12 weeks. All rats were sacrificed, and the heart and lung tissues were collected at week 20. The experiment was conducted in accordance with guidelines of the Committee on the Care and Use of Laboratory Animals of the First Affiliated Hospital, Henan University of Traditional Chinese Medicine, Zhengzhou, People's Republic of China. The study protocol was approved by the Experimental Animal Care and Ethics Committee of the First Affiliated Hospital (2012HLD-0001), Henan University of Traditional Chinese Medicine, Zhengzhou, People's Republic of China.

The components of BJF were as follows: AR 15 g, PR 15 g, CR 15 g, AMR 12 g, Po 12 g, FTB 9 g, Pheretima 12 g, MOC 9 g, CRP 9 g, ATR 9 g, AJH 15 g, and EH 6 g. The herbs were identified and prepared in fluid extract according to the standard operating procedure of the Department of Pharmaceutics of the First Affiliated Hospital, Henan University of Traditional Chinese Medicine, Zhengzhou, People's Republic of China.

Respiratory data collection

Respiratory data were collected by unrestrained pulmonary function testing plethysmography (Buxco Inc., Wilmington, NC, USA) conducted every 4th week from weeks 0 to 20. Buxco air flow transducers were connected to the chambers and to a reference chamber to compensate for pressure changes. Each chamber was calibrated to its respective transducer. We focused on three measures: tidal volume (TV), peak expiratory flow (PEF), and 50% TV expiratory flow.

Histological analyses

Heart and lung tissue samples were fixed in 10% formalin neutral buffer solution for 24 hours and then embedded in paraffin before being sliced into 4 μm sections. For histological examination, sections were stained with Mayer's hematoxylin and then with 1% eosin alcohol solution (hematoxylin and eosin staining). Samples were inspected with the aid of an Olympus BX51 microscope (Tokyo, Japan).

Bronchia, lung injury, and bronchiole stenosis were observed under an optical microscope. Alveolar number, alveolar diameter, small pulmonary vessels, and bronchial wall thickness were measured using Image-Pro Plus® 6.0 software (Media Cybernetics, Rockville, MD, USA). The morphometric analysis at the light microscopic level was conducted by an investigator blinded to the study protocol.

For immunohistochemical analysis, the right ventricle and lung tissue sections were transferred to gelatin-coated slides and then deparaffinized and rehydrated. The tissue slices were washed with 0.3% Triton X-100 in phosphate buffer (PB) and quenched with endogenous peroxidase (3% hydrogen peroxide). The sections were incubated with phosphate-buffered saline containing normal goat serum to reduce nonspecific reactions. Then, tissue sections were incubated overnight at 4°C with 1:300 dilutions of primary antibodies (Santa Cruz Biotechnology) against ET-1, TGF-β, VEGF, bFGF, MMP-2, MMP-9, TIMP-1, IL-6, IL-10, TNF-α, soluble TNF-α receptor 2, and collagens I, III, and IV in the presence of 2.5% bovine serum albumin. Slices were washed with phosphate buffer and incubated with the secondary antibody (Biocare Medical, Concord, CA, USA) for 2 hours. Immune complexes were visualized using the Catalyzed Signal Amplification System (Dako Denmark A/S, Glostrup, Denmark). Sections also were counter-stained with hematoxylin. Samples were inspected and measured using Image-Pro Plus® 6.0 software (Media Cybernetics).

Right ventricular hypertrophy index

After removing the arterial and adipose tissue on the epicardium, the right ventricle (RV), left ventricle (LV), and interventricular septum (S) were separated and weighed. The right ventricular hypertrophy index (RVHI) was calculated using the equation:

$$RVHI = RV/(LV + S).^{34} \quad (2)$$

Myocardial ultrastructure

The right ventricle was fixed with 3% glutaraldehyde, then 1% osmium tetroxide, and dehydrated. Through epoxy resin embedding and deployment of a hardener, accelerator, and growth agent, ultrathin sections of 70 nm thickness were cut and stained with uranyl acetate. Changes in the muscular fibers and mitochondria of the myocardial ultrastructure were observed with transmission electron microscopy.

Real-time reverse transcriptase polymerase chain reaction analysis

Total RNA was extracted from the lung tissues. Samples were reverse transcribed using a first-strand cDNA synthesis kit (Thermo Fisher Scientific, Waltham, MA, USA). Synthesized cDNA was used in real-time reverse transcriptase polymerase chain reaction (Bio-Rad Laboratories Inc., Hercules, CA,

USA) experiments. Specificity was confirmed by electrophoretic analysis of the reaction products and inclusion of template- or reverse transcriptase-free controls. Glyceraldehyde-3-phosphate dehydrogenase and hypoxanthine guanine phosphoribosyl transferase cDNA were used as an internal standard.

Statistical analysis

Values are expressed as mean ± standard error of mean. Statistical differences between groups were analyzed by one-way analysis of variance with the SPSS 19.0 software package (IBM Corporation, Armonk, NY, USA).

Results and discussion

Candidate compounds screening

In most cases, oral administration is the most predominant way to deliver drugs to systemic circulation for patients in TCM therapy; however, most compounds in herbs fail to reach to their cellular targets because they lack suitable pharmacokinetic properties, such as high oral bioavailability.[35] In addition, drug-like compounds contain functional groups and have physical properties that are consistent with clinical drugs.[20] Thus, a combination of OB screening and drug-likeness property evaluation was used to determine whether a compound was pharmaceutically active in the complex herbal mixture. Pheretima, an herbal constituent of BJF, was excluded because all of its compounds showed poor OB or drug-likeness indices. Then, 131 potential ingredients with OB ≥30% and drug-likeness index ≥0.18 were obtained from the eleven herbs. Additionally, we found that 14 molecules with low OB (≤30%) or drug-likeness indices (≤0.18) were the most abundant constituents and possessed extensive pharmacological activities.[21–29] Thus, these 14 ingredients also were included in the candidate active compounds for further target prediction and network analysis. Finally, 145 compounds of the eleven herbs were regarded as "active compounds", including the 131 readily absorbed compounds and the 14 pharmacologically active compounds (Table 1). The number of candidate active compounds in AR, PR, CR, AMR, Po, FTB, MOC, CRP, ATR, AJH, and EH was 20, 12, 24, 9, 16, 8, 2, 8, 19, 20, and 27, respectively. Among these, diosgenin, icariin, and nobiletin, which are the principal active compounds of PR, EH, and CRP, have been demonstrated to have extensive pharmacological activities as predicted in the current study.[27,36,37] Similarly, luteolin and quercetin, which occur widely in herbs such as AR, ATR, AJH, and EH, have been shown to overcome OB barriers by inhibition of permeability glycoprotein and possess a broad spectrum of biological and pharmacological properties.[38,39]

Target identification

In general, TCM formula contains tens of thousands of active compounds, which provide bright prospects for prevention and treatment of complex diseases in a synergistic manner. To illuminate the detailed mechanisms of the effects of TCM formula, it is crucial to uncover the therapeutic targets of active compounds contained in the formulas. In this study, a pharmacophore modeling technique was applied to search potential targets based on the "candidate compounds". A total of 175 candidate targets were identified for the 131 candidate compounds; however, 14 candidate compounds had no candidate target under this criterion (Table S2). Finally, 131 candidate compounds yielded 175 potential targets, and the connections between them reached 1,849.

The numbers of potential targets connected by AR, PR, CR, AMR, Po, FTB, MOC, CRP, ATR, AJH, and EH were 134, 70, 92, 33, 36, 56, 43, 56, 121, 99, and 140, respectively. Although the numbers of each herb-related target were different, there was a significant target overlap between the eleven herbs. These results indicated that each herb could connect with similar multitargets, suggesting the potential synergistic effects among them. For example, tangshenoside II (from CR), atractylenolide III (from AMR), honokiol (from MOC), and nobiletin (from CRP) have been shown to attenuate the function of nitric oxide synthase, which plays an important role in regulating blood pressure and, thus, ameliorate coronary artery vascular tone and local or systemic inflammatory disorders.[22,23,37,40]

Compound–target network

TCM formulas are regarded as multicomponent therapeutics, which means that the active compounds of the herbal drugs simultaneously interact with the same or different targets. To understand the drug action at a systems level, the network theory was used to uncover the underlying interactions between the candidate compounds and targets (Table S3). Here, we mapped the compounds from the eleven herbs and targets onto compound–target networks. Figure 1 shows a global view of the compound–target network with color-coded nodes: herb (square, orange), candidate compounds (rhombus, blue), and candidate targets (ellipse, green). The network consisted of 1,849 compound–target interactions connecting the 131 candidate compounds to 175 targets, resulting in an average number of targets per active compound

Table 1 Chemical information of 165 candidate compounds and their network parameters

Herb ID	Molecule name	Degree	OB	DL	InChIKey
AR.1	(3S,8S,9S,10R,13R,14S,17R)-10,13-dimethyl-17-[(2R,5S)-5-propan-2-yloctan-2-yl]-2,3,4,7,8,9,11,12,14,15,16,17-dodecahydro-1H-cyclopenta[a]phenanthren-3-ol	3	36.2	0.783	KLEXDBGYSOIREE-UIFQYPGESA-N
AR.2	9,10-Dimethoxypterocarpan-3-O-β-D-glucoside	6	36.7	0.924	PCIXSTFFMHVOMF-PBGSHFJYSA-N
AR.3	(6aR,11aR)-9,10-dimethoxy-6a,11a-dihydro-6H-benzofurano[3,2-c]chromen-3-ol	34	64.3	0.425	UOVGCLXUTLXAEC-WFASDCNBSA-N
AR.4	Bifendate	14	31.1	0.666	JMZOMFYRADAWOG-UHFFFAOYSA-N
AR.5	Formononetin	36	69.7	0.212	HKQYGTCOTHHOMP-UHFFFAOYSA-N
AR.6	Isoflavone	0	110.0	0.296	JNSVNRWHSLLCBG-LLVKDONJSA-N
AR.7	Calycosin	25	47.8	0.243	ZZAJQOPSWWVMBI-UHFFFAOYSA-N
AR.8	Kaempferol	55	41.9	0.241	IYRMWMYZSQPJKC-UHFFFAOYSA-N
AR.9	FA	3	69.0	0.706	OVBPIULPVIDEAO-LBPRGKRZSA-N
AR.10	(3R)-3-(2-hydroxy-3,4-dimethoxyphenyl)chroman-7-ol	0	67.7	0.265	NQRBAPDEZYMKFL-NSHDSACASA-N
AR.11	Isomucronulatol-7,2′-di-O-glucosiole	1	49.3	0.621	NHOPAJCVMDIGBN-MEPKZADGSA-N
AR.12	Quercetin	87	46.4	0.275	REFJWTPEDVJJIY-UHFFFAOYSA-N
AR.13	1,7-Dihydroxy-3,9-dimethoxy pterocarpene	16	39.0	0.479	RVGZSUMTFIEORY-UHFFFAOYSA-N
AR.14	Mairin	4	55.4	0.776	QGJZLNKBHJESQX-FZFNOLFKSA-N
AR.15	Jaranol	21	50.8	0.291	BJBUTJQYZDYRMJ-UHFFFAOYSA-N
AR.16	Hederagenin	34	36.9	0.751	KZJWDPNRJALLNS-CQXWNKEUSA-N
AR.17	Isorhamnetin	36	49.6	0.306	IZQSVPBOUDKVDZ-UHFFFAOYSA-N
AR.18	3,9-di-O-methylnissolin	35	53.7	0.476	RFFNFQZKHNKOPO-BBRMVZONSA-N
AR.19	5′-Hydroxyiso-muronulatol-2′,5′-di-O-glucoside	0	41.7	0.693	SRVGYVIWVOOXQO-FQRJZKGRSA-N
AR.20	7-O-methylisomucronulatol	47	74.7	0.298	BLHQCBJSTMDZQA-LBPRGKRZSA-N
PR.1	Beta-sitosterol	51	36.9	0.751	KZJWDPNRJALLNS-VJSFXXLFSA-N
PR.2	Sitosterol	6	36.9	0.751	KZJWDPNRJALLNS-ZFVHJZABSA-N
PR.3	Diosgenin	13	80.9	0.810	WQLVFSAGQJTQCK-VKROHFNGSA-N
PR.4	DFV	24	32.8	0.183	FURUXTVZLHCCNA-AWEZNQCLSA-N
PR.5	Baicalein	33	33.5	0.209	FXNFHKRTJBSTCS-UHFFFAOYSA-N
PR.6	3′-Methoxydaidzein	21	48.6	0.243	MUYAUELJBWQNDH-UHFFFAOYSA-N
PR.7	Methylprotodioscin_qt	2	35.1	0.859	ZHIBERYBFVVFNK-WMMDDPCFSA-N
PR.8	(2R)-7-hydroxy-2-(4-hydroxyphenyl)chroman-4-one	28	71.1	0.183	FURUXTVZLHCCNA-CQSZACIVSA-N
PR.9	4′,5-Dihydroxyflavone	20	48.6	0.186	OKRNDQLCMXUCGG-UHFFFAOYSA-N
PR.10	Sibiricoside A_qt	3	35.3	0.862	ZSYOERSNLZAHLT-BBLSMLIUSA-N
PR.11	(+)-Syringaresinol-O-beta-D-glucoside	1	43.4	0.767	WEKCEGQSIIQPAQ-QVYKXMJQSA-N
PR.12	Zhonghualiaoine 1	1	34.7	0.776	RSZFVFRVXKODEL-WYWHROKUSA-N
CR.1	Luteolin	41	36.2	0.246	IQPNAANSBPBGFQ-UHFFFAOYSA-N
CR.2	Stigmasterol	44	43.8	0.757	HCXVJBMSMIARIN-PHZDYDNGSA-N
CR.3	Poriferasta-7,22E-dien-3beta-ol	6	43.0	0.756	JZVFJDZBLUFKCA-INYURWPISA-N
CR.4	Perlolyrine	12	65.9	0.275	KFUCYPGCMLPUMT-UHFFFAOYSA-N
CR.5	Diop	8	43.6	0.392	IJFPVINAQGWBRJ-UHFFFAOYSA-N
CR.6	ZINC03978781	6	43.8	0.756	HCXVJBMSMIARIN-NKMAIEQZSA-N
CR.7	7-Methoxy-2-methyl isoflavone	45	42.6	0.199	XRGWZIGGCNSFRY-UHFFFAOYSA-N
CR.8	Spinasterol	6	43.0	0.755	JZVFJDZBLUFKCA-FXIAWGAOSA-N

CR.9	Chrysanthemaxanthin	1	38.7	0.584	JRHJXXLCNATYLS-HYHFCDFPSA-N
CR.10	Frutinone A	27	65.9	0.342	RFWULRHBGYKEEZ-UHFFFAOYSA-N
CR.11	Taraxerol	2	38.4	0.767	GGGUGZHBAOMSFJ-GADYQYKKSA-N
CR.12	Stigmast-7-enol	4	37.4	0.751	YSKVBPGQYRAUQO-UBCZCFGNSA-N
CR.13	3-beta-Hydroxymethyllenetanshiquinone	30	32.2	0.409	RUJKJFRMCYQMLH-ZDUSSCGKSA-N
CR.14	Methyl icosa-11,14-dienoate	6	39.7	0.229	GWJCFAOQCNNFAM-ZDVGBALWSA-N
CR.15	Tangshenoside III_qt	24	5.0	0.450	AKICIBIGIPCIKV-SFECMWDFSA-N
CR.16	5alpha-Stigmastan-3,6-dione	2	33.1	0.790	HMMVBUVVQLUGQA-CFLIYZTGSA-N
CR.17	7-(beta-Xylosyl)cephalomannine_qt	1	38.3	0.286	YVFWOWYGCXXKFY-IICLVWGGSA-N
CR.18	Daturilin	3	50.4	0.768	QUGZOXCXHGEACS-ZFEQYVDASA-N
CR.19	Glycitein	25	50.5	0.238	DXYUAIFZCFRPTH-UHFFFAOYSA-N
CR.20	Spinoside A	0	40.0	0.403	KNKOUUNHYIXOAK-OCCINUARSA-N
CR.21	(8S,9S,10R,13R,14S,17R)-17-[(E,2R,5S)-5-ethyl-6-methylhept-3-en-2-yl]-10,13-dimethyl-1,2,4,7,8,9,11,12,14,15,16,17-dodecahydrocyclopenta[a]phenanthren-3-one	5	45.4	0.762	XWDAKKDQJHVMKG-LPJPOILFSA-N
CR.22	Tangshenoside II	11	19.5	0.317	MATKEAOBTGAMFZ-WKDOMPITSA-N
CR.23	Tangshenoside II_qt	13	51.7	0.064	DFUGWNKUOJIKNF-MRVPVSSYSA-N
CR.24	11-Hydroxyrankinidine	4	40.0	0.662	FALAMCOLIJTCTR-XAVCKHEUSA-N
AMR.1	12-Senecioyl-2E,8E,10E-atractylentriol	0	62.4	0.223	UJHAKGDWVZIMIT-PKPRIEKHSA-N
AMR.2	14-Acetyl-12-senecioyl-2E,8E,10E-atractylentriol	0	60.3	0.305	CQDVFBMTEZFKKY-JAPNHWDDSA-N
AMR.3	14-Acetyl-12-senecioyl-2E,8Z,10E-atractylentriol	4	63.4	0.300	CQDVFBMTEZFKKY-PUYRJQRLSA-N
AMR.4	α-Amyrin	0	39.5	0.763	FSLPMRQHCOLESF-FRCIEAHOSA-N
AMR.5	(3S,8S,9S,10R,13R,14S,17R)-10,13-dimethyl-17-[(2R,5S)-5-propan-2-yloctan-2-yl]-2,3,4,7,8,9,11,12,14,15,16,17-dodecahydro-1H-cyclopenta[a]phenanthren-3-ol	3	36.2	0.783	KLEXDBGYSOIREE-UIFQYPGESA-N
AMR.6	Atractylenolide I	12	37.4	0.149	ZTVSGQPHMUYCRS-SWLSCSKDSA-N
AMR.7	Atractylenolide III	10	68.1	0.171	FBMORZZOJSDNRQ-GLQYFDAESA-N
AMR.8	3β-Acetoxyatractylone	20	54.1	0.219	YYGOPZCCRBWMBK-ZOBUZTSGSA-N
AMR.9	8β-Ethoxy atractylenolide III	12	36.0	0.211	JATCNILBQFTWFJ-XKQJLSEDSA-N
Po.1	(2R)-2-[(3S,5R,10S,13R,14R,16R,17R)-3,16-dihydroxy-4,4,10,13,14-pentamethyl-2,3,5,6,12,15,16,17-octahydro-1H-cyclopenta[a]phenanthren-17-yl]-6-methylhept-5-enoic acid	4	30.9	0.813	XSLKAKROJKMHIT-WIUKAADNSA-N
Po.2	Trametenolic acid	4	38.7	0.802	NBSBUIQBEPROBM-QPOZJWKMSA-N
Po.3	7,9(11)-Dehydropachymic acid	1	35.1	0.811	RWIALJIVPUCERT-DRCQUEPLSA-N
Po.4	Cerevisterol	4	38.0	0.771	ARXHRTZAVQOQEU-BRVLHLJYSA-N
Po.5	(2R)-2-[(3S,5R,10S,13R,14R,16R,17R)-3,16-dihydroxy-4,4,10,13,14-pentamethyl-2,3,5,6,12,15,16,17-octahydro-1H-cyclopenta[a]phenanthren-17-yl]-5-isopropyl-hex-5-enoic acid	2	31.1	0.815	LADJWZMBZBVBSB-YEXRKOARSA-N
Po.6	Ergosta-7,22E-dien-3beta-ol	4	43.5	0.719	QOXPZVASXWSKKU-UEIWAABPSA-N
Po.7	Ergosterol peroxide	4	40.4	0.813	PIENIXCJUGJKPI-JYJMTLRPSA-N
Po.8	(2R)-2-[(5R,10S,13R,14R,16R,17R)-16-hydroxy-3-keto-4,4,10,13,14-pentamethyl-1,2,5,6,12,15,16,17-octahydrocyclopenta[a]phenanthren-17-yl]-5-isopropyl-hex-5-enoic acid	0	38.3	0.820	KPKYWYZPIVAHKU-WMNQUVFJSA-N
Po.9	3beta-Hydroxy-24-methylene-8-lanostene-21-oic acid	2	38.7	0.810	UGMQOYZVOPASJF-OXUZYLMNSA-N

(*Continued*)

Table 1 (*Continued*)

Herb ID	Molecule name	Degree	OB	DL	InChIKey
Po.10	Pachymic acid	1	33.6	0.811	VDYCLYGKCGVBHN-KVPCPLELSA-N
Po.11	Poricoic acid A	2	30.6	0.762	KVAQLXUMUVEKGR-SMFZDKLCSA-N
Po.12	Poricoic acid B	2	30.5	0.746	NXAZWYWJZDFISF-KXGBKNTBSA-N
Po.13	Poricoic acid C	1	38.2	0.746	QFVFCBZDUKVXLR-PKSIZLAPSA-N
Po.14	Hederagenin	34	36.9	0.751	KZJWDPNRJALLNS-CQXWNKEUSA-N
Po.15	Ergosterol	6	14.3	0.723	DNVPQKQSNYMLRS-APGDWVJJSA-N
Po.16	Dehydroeburicoic acid	0	44.2	0.835	WZWOZRZYBSGARK-NUPWKHSHSA-N
FTB.1	beta-Sitosterol	51	36.9	0.751	KZJWDPNRJALLNS-VJSFXXLFSA-N
FTB.2	Pelargonidin	25	38.0	0.212	SAURRTSFHXYOSN-UHFFFAOYSA-N
FTB.3	Peimisine	4	57.4	0.806	KYELXPJVGNZIGC-GKFGJCLESA-N
FTB.4	Zhebeiresinol	16	58.7	0.194	AUXYOVQIZNPKSO-KKFJDGPESA-N
FTB.5	Ziebeimine	2	64.2	0.705	OEJGVNMSFPGDPP-BDFZTFKFSA-N
FTB.6	6-Methoxyl-2-acetyl-3-methyl-1,4-naphthoquinone-8-O-beta-D-glucopyranoside	10	33.3	0.573	GVMOOQOCLYWVKF-BNCZOOBYSA-N
FTB.7	Chaksine	1	65.6	0.665	CGGAHJGHSHWGLE-WJQMWINMSA-N
FTB.8	Peiminoside_qt	3	11.8	0.668	IUKLSMSEHKDIIP-FWSIRKJPSA-N
MOC.1	Eucalyptol	37	60.6	0.322	PDRGHUMCVRDZLQ-FUHWJXTLSA-N
MOC.2	Neohesperidin	23	57.4	0.271	YNYGAMJOLICYES-CQSZACIVSA-N
CRP.1	Anthocyanidin	0	45.6	0.190	YLJQHJNWIHUOKW-UHFFFAOYSA-N
CRP.2	Sitosterol	6	36.9	0.751	KZJWDPNRJALLNS-ZFVHJZABSA-N
CRP.3	Naringenin	33	59.3	0.211	FTVWIRXFELQLPI-ZDUSSCGKSA-N
CRP.4	5,7-Dihydroxy-2-(3-hydroxy-4-methoxyphenyl)chroman-4-one	26	47.7	0.272	AIONOLUJZLIMTK-CQSZACIVSA-N
CRP.5	Naringin	2	6.9	0.778	DFPMSGMNTNDNHN-ZPHOTFPESA-N
CRP.6	Citromitin	23	86.9	0.514	LTRBUBSPQISFFL-CQSZACIVSA-N
CRP.7	Nobiletin	30	61.7	0.517	MRIAQLRQZPPODS-UHFFFAOYSA-N
CRP.8	Hesperidin	2	13.3	0.667	QUQPHWDTPGMPEX-QJBIFVCTSA-N
ATR.1	Luteolin	41	36.2	0.246	IQPNAANSBPBGFQ-UHFFFAOYSA-N
ATR.2	Quercetin	87	46.4	0.275	REFJWTPEDVJJIY-UHFFFAOYSA-N
ATR.3	Isorhamnetin	36	49.6	0.306	IZQSVPBOUDKVDZ-UHFFFAOYSA-N
ATR.4	beta-Sitosterol	51	36.9	0.751	KZJWDPNRJALLNS-VJSFXXLFSA-N
ATR.5	Kaempferol	55	41.9	0.241	IYRMWMYZSQPJKC-UHFFFAOYSA-N
ATR.6	Galangin	26	45.6	0.207	VCCRNZQBSJXYJD-UHFFFAOYSA-N
ATR.7	ZINC03978781	6	43.8	0.756	HCXVJBMSMIARIN-NKMAIEQZSA-N
ATR.8	Epifriedelanol acetate	2	31.2	0.740	NXKDUDYUASKXAY-BATOFVLWSA-N
ATR.9	Spinasterol	6	43.0	0.755	JZVFJDZBLUFKCA-FXIAWGAOSA-N
ATR.10	5,7-Dihydroxy-2-(3-hydroxy-4-methoxyphenyl)chroman-4-one	26	47.7	0.272	AIONOLUJZLIMTK-CQSZACIVSA-N
ATR.11	16beta,17-Dihydroxy-(-)-kauran-19-ate-beta-D-glucose ester_qt	5	56.7	0.427	MRBLTWPEPGRXQN-SYHVJVMTSA-N
ATR.12	Astin C	0	34.6	0.514	MUWSKAXEQCKXQN-CDEOPILDSA-N
ATR.13	Astin D	2	52.8	0.771	MWFWIMVUPUHHEG-ICBNADEASA-N
ATR.14	(13S)-13-[(4-o-acetyl-6-deoxy-alpha-l-mannopyranosyl)oxy]-labda-8(20),14-diene	1	36.8	0.681	ZTNQJRLNKSLKMO-GSIQLPOHSA-N
ATR.15	[(2S,3R,4R,5R,6S)-2-[(1S)-1-[2-[(1S,4aS,8aS)-5,5,8a-trimethyl-2-methylene-decalin-1-yl]ethyl]-1-methyl-prop-2-enoxy]-4,5-dihydroxy-6-methyl-tetrahydropyran-3-yl] acetate	1	37.0	0.680	QKJSTDJCPDBOHF-GWMYBZPOSA-N

ATR.16	(13S)-13-[(2,4-di-o-acetyl-6-deoxy-alpha-l-mannopyr-anosyl)oxy]labda-8(20),14-diene	1	37.8	0.751	JJBGTRVRWMWIPE-ZWULDHRZSA-N
ATR.17	Rabdosinatol	5	30.9	0.415	NTFFIALEDUMPAM-ULBKSSDQSA-N
ATR.18	Shionone	3	38.9	0.731	HXPXUNQUXCHJLL-LZQQOHPBSA-N
ATR.19	Shionoside C	0	30.9	0.860	WMCBNRYIQQZLBT-HPTRTUHESA-N
AJH.1	Quercetin	87	46.4	0.275	REFJWTPEDVJJIY-UHFFFAOYSA-N
AJH.2	Kaempferol	55	41.9	0.241	IYRMWMYZSQPJKC-UHFFFAOYSA-N
AJH.3	(4aS,6aR,6aS,6bR,8aR,10R,12aR,14bS)-10-hydroxy-2,2,6a,6b,9,9,12a-heptamethyl-1,3,4,5,6,6a,7,8,8a,10,11,12,13,14b-tetradecahydropicene-4a-carboxylic acid	3	32.0	0.757	MIJYXULNPSFWEK-KDQGZELNSA-N
AJH.4	Bergenin	10	14.1	0.342	YWJXCIXBAKGUKZ-HJJNZUOJSA-N
AJH.5	Diop	8	43.6	0.392	IJFPVINAQGWBRJ-UHFFFAOYSA-N
AJH.6	Laricitrin	22	35.4	0.342	CFYMYCCYMJIYAB-UHFFFAOYSA-N
AJH.7	Ardisianoside K_qt	2	32.0	0.626	DLWHFHBRYSITBI-WGIDJJHTSA-N
AJH.8	Triterpenoid glycoside 1_qt	2	34.1	0.631	UBWMMEPLQFWYCH-GZAMYCOFSA-N
AJH.9	Maesanin	6	42.8	0.351	WVHQJXPRVZBEFP-SREVYHEPSA-N
AJH.10	Rapanone	0	34.2	0.238	AMKNOBHCKRZHIO-UHFFFAOYSA-N
AJH.11	tri-O-methylnorbergenin	10	33.2	0.410	RGHGUQJYNLPWPT-GVMTXOEMSA-N
AJH.12	Triterpene glycoside 4_qt	1	41.4	0.631	UBWMMEPLQFWYCH-RMXBMUOASA-N
AJH.13	Triterpenoid glycoside 3_qt	1	44.0	0.601	WTFUHAGPAIREPL-RYZHOHRSSA-N
AJH.14	2,5-Dihydroxy-3-[(10Z)-pentadec-10-en-1-yl][1,4]benzoquinone	0	34.7	0.603	OZOJZESTKHHHQP-WAYWQWQTSA-N
AJH.15	2,5-Dihydroxy-3-[(10Z)-pentadec-10-en-1-yl]cyclohexa-2,5-diene-1,4-dione	1	37.3	0.320	YRIWERDENGDRIR-WAYWQWQTSA-N
AJH.16	2-Hydroxy-5-methoxy-3-pentadecaenylbenzoquinone	1	41.6	0.315	GSFLASJBASRJKZ-HYPNTESJSA-N
AJH.17	5-Ethoxy-2-hydroxy-3-[(10Z)-pentadec-10-en-1-yl][1,4]benzoquinone	2	42.8	0.383	YQDOWDWMMZKLQR-FPLPWBNLSA-N
AJH.18	5-Ethoxy-2-hydroxy-3-[(8Z)-tridec-8-en-1-yl][1,4]benzoquinone	5	43.2	0.296	XELCDMYKAGKICS-FPLPWBNLSA-N
AJH.19	Ardisianone A	7	44.2	0.249	WNZXOLJKBYUFDZ-ZFYPLVIYSA-N
AJH.20	Ardisianone B	11	60.9	0.198	TYEYBRGUMMKRGI-ZHANPKHBSA-N
EH.1	Luteolin	41	36.2	0.246	IQPNAANSBPBGFQ-UHFFFAOYSA-N
EH.2	Quercetin	87	46.4	0.275	REFJWTPEDVJJIY-UHFFFAOYSA-N
EH.3	Sitosterol	6	36.9	0.751	KZJWDPNRJALLNS-ZFVHJZABSA-N
EH.4	Kaempferol	55	41.9	0.241	IYRMWMYZSQPJKC-UHFFFAOYSA-N
EH.5	Magnograndiolide	5	63.7	0.188	VHFXPBHLQOPQHJ-ABBQYLIMSA-N
EH.6	24-Epicampesterol	4	37.6	0.714	SGNBVLSWZMBQTH-ZRUUVFCLSA-N
EH.7	Linoleyl acetate	8	42.1	0.198	KFXARGMQYWECBV-ZDVGBALWSA-N
EH.8	Poriferast-5-en-3beta-ol	5	36.9	0.750	KZJWDPNRJALLNS-FBZNIEFRSA-N
EH.9	DFV	24	32.8	0.183	FURUXTVZLHCCNA-AWEZNQCLSA-N
EH.10	Chrysoeriol	24	35.9	0.274	SCZVLDHREVKTSH-UHFFFAOYSA-N
EH.11	8-Isopentenyl-kaempferol	34	38.0	0.395	NADCVNHITZNGJU-UHFFFAOYSA-N
EH.12	Olivil	17	62.2	0.406	BVHIKUCXNBQDEM-XMCHAPAWSA-N
EH.13	Anhydroicaritin	39	45.4	0.438	TUUXBSASAQJECY-UHFFFAOYSA-N
EH.14	C-Homoerythrinan, 1,6-didehydro-3,15,16-trimethoxy-, (3.beta.)-	44	39.1	0.495	VFNBFPRWBICVGZ-JXFKEZNVSA-N
EH.15	Yinyanghuo A	10	57.0	0.767	ZAUWPDSVLSOCDG-SFHVURJKSA-N
EH.16	Yinyanghuo C	19	45.7	0.502	GPXYBBZISZKRAH-UHFFFAOYSA-N

(*Continued*)

Table 1 (*Continued*)

Herb ID	Molecule name	Degree	OB	DL	InChIKey
EH.17	Yinyanghuo D	19	14.0	0.380	PFQMUQWFRINBBG-UHFFFAOYSA-N
EH.18	Yinyanghuo E	21	51.6	0.547	FIKLOAGOJKGOFT-UHFFFAOYSA-N
EH.19	6-Hydroxy-11,12-dimethoxy-2,2-dimethyl-1,8-dioxo-2,3,4,8-tetrahydro-1H-isochromeno[3,4-h]isoquinolin-2-ium	16	60.6	0.657	FUBYUUKASUJMSZ-UHFFFAOYSA-N
EH.20	8-(3-Methylbut-2-enyl)-2-phenyl-chromone	30	48.5	0.251	FMPOBQILEGSRSJ-UHFFFAOYSA-N
EH.21	Anhydroicaritin	25	28.3	0.593	PPCHTBBOSVKORE-UHFFFAOYSA-N
EH.22	Anhydroicaritin-3-O-alpha-L-rhamnoside	1	41.6	0.610	TZJALUIVHRYQQB-YPRONELTSA-N
EH.23	1,2-bis(4-Hydroxy-3-methoxyphenyl)propan-1,3-diol	20	52.3	0.221	DFUOJBWSSODTR-SJCJKPOMSA-N
EH.24	Hexandraside E	27	13.6	0.596	SLUGZPRLJCECEX-YVBMKHBZSA-N
EH.25	Icariin	1	41.6	0.611	TZJALUIVHRYQQB-XLRXWWTNSA-N
EH.26	Icariside A7	5	31.9	0.856	HNMHZSRVQJZGPQ-PUIBNRJISA-N
EH.27	Icariside I	27	21.9	0.848	IYCPMVXIUPYNHI-RBOMYRCTSA-N

Note: "_qt", the compound with glycosyl groups is deglycosylated by the rule of glycosidase hydrolysis reaction.

Abbreviations: OB, oral bioavailability; DL, drug-likeness; AR, Astragali Radix; PR, Polygonati Rhizoma; CR, Codonopsis Radix; AMR, Atractylodis Macrocephalae Rhizoma; Po, Poria; FTB, Fritillariae Thunbergii Bulbus; MOC, Magnoliae Officinalis Cortex; CRP, Citri Reticulatae Pericarpium; ATR, Asteris Tatarici Radix; AJH, Ardisiae Japonicae Herba; EH, Epimedii Herba; FA, folic acid; DFV, liquiritigenin.

of 1.34. Among the 131 candidate compounds, 49 compounds possessed a degree (the number of target associated with it) larger than 15, with an average value of 14.1. This suggests that many compounds bind to multiple targets, thereby giving rise to polypharmacology. These compounds play important roles in the networks, which were selected to illustrate the pharmacological activities of BJF, such as the two highly connected nodes, quercetin (degree =87) and kaempferol (degree =55). For instance, quercetin was one of the largest hubs connecting to different targets. Quercetin had high affinities with peroxisome proliferator activated receptor gamma (PPARγ), nitric oxide synthase, inducible, prostaglandin G/H synthase 1/2 (also known as COX-1, -2), and estrogen receptor, which induce a complex pharmacological profile including anti-inflammatory, immunomodulatory, antioxidant, and antiproliferative effects, among others. Furthermore, these results also indicated that many target are cross-linked together in the compound–target network. For example, the androgen receptor, the most highly connected target, is linked to 79% (104 of 131) of the compounds, followed by the estrogen receptor (degree =93), prostaglandin G/H synthase 1/2 (degree =66), nitric oxide synthase, inducible (degree =56), dipeptidyl peptidase IV (degree =56), thrombin (degree =54), and PPARγ (degree =53). Interestingly, nitric oxide synthase, inducible, PPARγ, and prostaglandin G/H synthase 1/2 expression is correlated closely with inflammation and immune system activation.[41,42]

In an effort to illuminate the therapeutic mechanism of the 175 selected targets, we applied ClueGO, a Cytoscape plugin, to explore the biological interpretation of the potential targets,[43] and divided the results into three stratums: molecular function, the immune system processes, and the reactome analysis. As shown in Figure 2A, the main molecular functions were classified into four categories: oxidoreductase activity, mitogen-activated protein kinase (MAPK) activity, neurotransmitter receptor activity, and G-protein-coupled amine receptor activity. The large majority of targets were related to oxidoreductase and MAPK activities, which are the activities mainly responsible for COPD.[44,45] In Figure 2B, the immune system processes of the targets are associated mainly with positive regulation of myeloid leukocyte differentiation, T-cell lineage commitment, positive regulation of immune effector processes, and the toll-like receptor 10 signaling pathway. Consequently, the reactome of the targets are related to activation of the activator protein-1 family of transcription factors, MAPK targets/nuclear events mediated by MAPK, and activation of MMPs (Figure 2C).

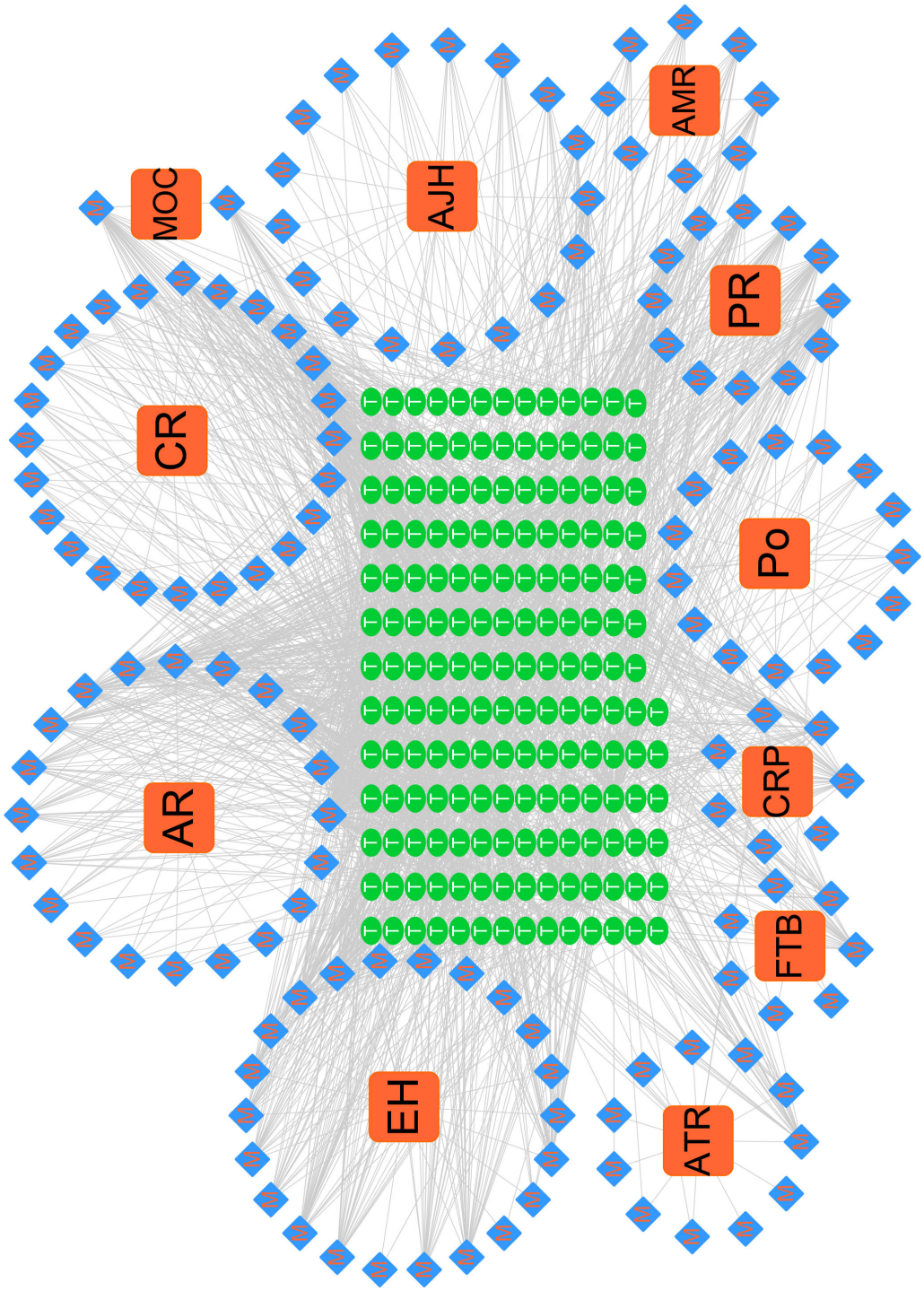

Figure 1 Compound–target network (C–T network).
Notes: The C–T network was built by linking the candidate compounds (rhombus, blue) of eleven herbs (square, orange) and all their candidate targets (ellipse, green). The C–T network consists of eleven herbs and 1,849 compound–target interactions connecting the 131 candidate compounds to 175 targets.
Abbreviations: T, target; M, molecular; AR, Astragali Radix; PR, Polygonati Rhizoma; CR, Codonopsis Radix; AMR, Atractylodis Macrocephalae Rhizoma; Po, Poria; FTB, Fritillariae Thunbergii Bulbus; MOC, Magnoliae Officinalis Cortex; CRP, Citri Reticulatae Pericarpium; ATR, Asteris Tatarici Radix; AJH, Ardisiae Japonicae Herba; EH, Epimedii Herba.

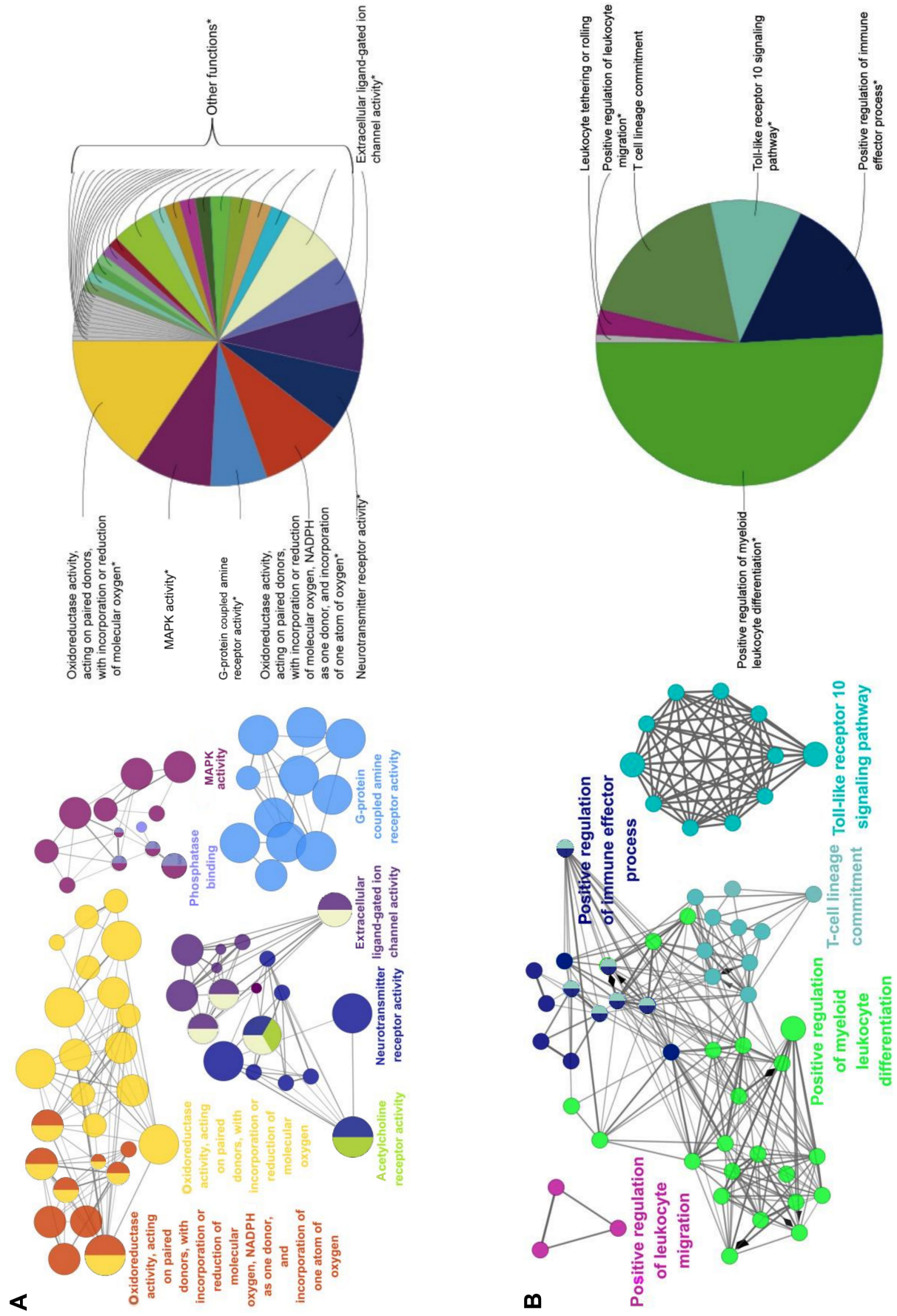
A
Oxidoreductase activity, acting on paired donors, with incorporation or reduction of molecular oxygen, NADPH as one donor, and incorporation of one atom of oxygen
Oxidoreductase activity, acting on paired donors, with incorporation or reduction of molecular oxygen
Phosphatase binding
MAPK activity
G-protein coupled amine receptor activity
Extracellular ligand-gated ion channel activity
Neurotransmitter receptor activity
Acetylcholine receptor activity
Other functions*
Extracellular ligand-gated ion channel activity*
Oxidoreductase activity, acting on paired donors, with incorporation or reduction of molecular oxygen*
MAPK activity*
G-protein coupled amine receptor activity*
Oxidoreductase activity, acting on paired donors, with incorporation or reduction of molecular oxygen, NADPH as one donor, and incorporation of one atom of oxygen*
Neurotransmitter receptor activity*
B
Positive regulation of immune effector process
Toll-like receptor 10 signaling pathway
T-cell lineage commitment
Positive regulation of myeloid leukocyte differentiation
Positive regulation of leukocyte migration
Positive regulation of myeloid leukocyte differentiation*
Leukocyte tethering or rolling
Positive regulation of leukocyte migration*
T cell lineage commitment
Toll-like receptor 10 signaling pathway*
Positive regulation of immune effector process*

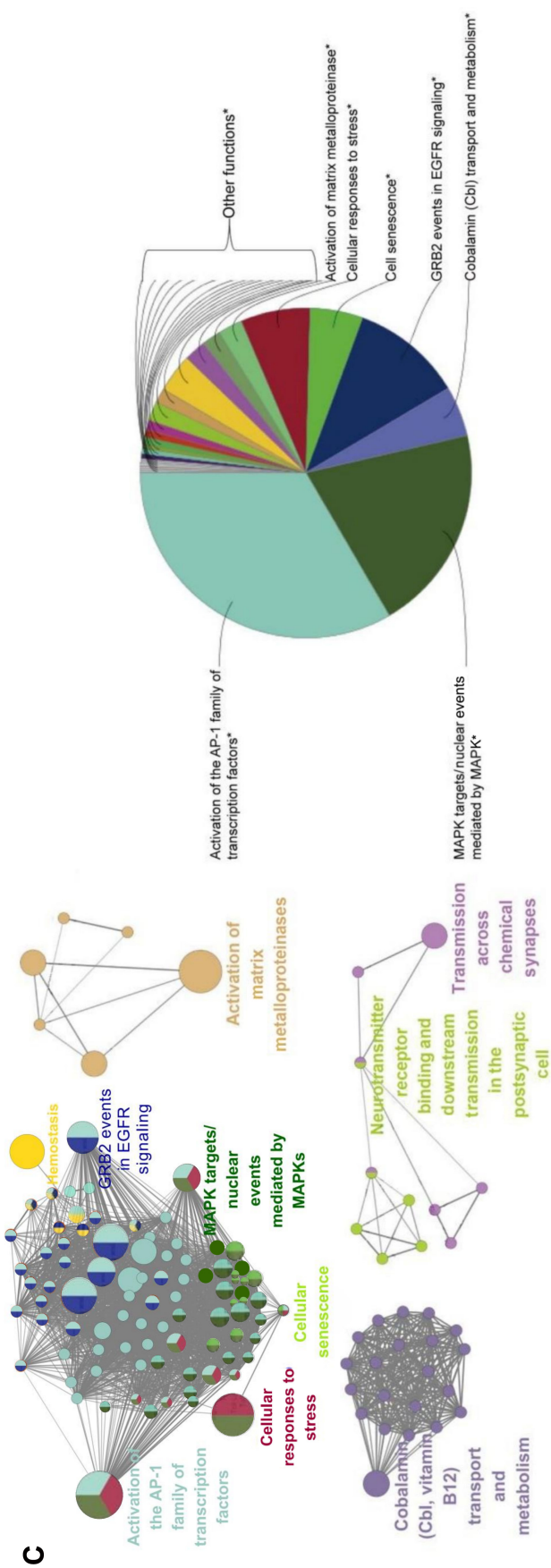

Figure 2 ClueGO analysis of the predicted targets.
Notes: Functionally grouped network with terms as nodes linked and functionally-related groups partially overlap. The node size represents the term enrichment significance. The node pie charts represent the molecular function, immune system processes, and reactome analysis of each target corresponding to their networks in this target set. The label of only the significant term per group is shown. (**A**) Representative molecular function interactions among targets. (**B**) Representative immune system processes interactions among targets. (**C**) Representative reactome analysis interactions among predicted targets. *Represents enrichment significance.
Abbreviations: AP-1, activator protein-1; EGFR,epidermal growth factor receptor; GRB2, growth factor receptor-bound protein 2; MAPK, mitogen-activated protein kinase; NADPH, nicotinamide adenine dinucleotide phosphate.

Multiple intermediate risk factors, such as chronic bronchitis, small-airway disease, and emphysema,[3,6,46] which might induce differences in protein expression, are incriminated in COPD etiology. Thus, a single compound or herb is probably insufficient for COPD therapy. From our results, common targets with multiple functions shared by the active compounds suggest that the BJF could possess synergistic therapeutic effects for COPD and possibly could be more effective than a single herb or compound.

Target–disease network

All of the 175 targets were projected into the DrugBank, Therapeutic Target, and PharmGkb databases to collect their related diseases. Then, 348 diseases belonging to 16 groups derived from the MeSH Browser (2014 MeSH) were obtained. Finally, the target–disease interactions are shown in the target–disease network (Figure 3). Interestingly, among these 348 diseases, we found that most of them belong to neoplasms (87/348), nervous system diseases (65/348), cardiovascular diseases (50/348), and nutritional and metabolic diseases (21/348), apart from respiratory tract diseases (26/348). This illustrated that BJF probably has effectiveness not only on respiratory diseases but also on these diseases. This is consistent with the use of Chinese medicines for the treatment of various diseases. For instance, PPARγ connected with inflammatory response and immunomodulatory activities in atherosclerosis, type 2 diabetes, inflammatory bowel disease, arthritis, asthma, COPD, and other airway diseases and, as a result, has the potential to become a therapeutic target for COPD and other diseases.[47–49] In the target–disease network, we also found that PPARγ connected with many of these diseases. In addition, to clarify further the relationship among the compounds, the targets, and the correlated diseases, experimental studies were conducted.

Effect of BJF on COPD and its comorbidity

In a previous study, BJF was confirmed to have beneficial clinical efficacy in COPD patients.[9] In addition, the target–disease network predicts that BJF has efficiency not only for the treatment of respiratory diseases but also for other diseases, such as nervous system and cardiovascular diseases. To test further this prediction, we next examined the effect of BJF on COPD rats and its comorbidity, ventricular hypertrophy.[50–52]

To determine the effect of BJF on COPD rats, the intragastric administration of BJF to rats was commenced 9 weeks after the administration of cigarette smoke, and lung mechanics and pulmonary histopathology were assessed. As shown in Figure 4, compared with the control rat, the TV, PEF, and 50% TV expiratory flow clearly decreased in the model rat from weeks 4 to 20, whereas, compared with the model rats, BJF had significantly increased the TV and PEF in the COPD rats at week 20. Furthermore, aminophylline, a classical bronchodilator, also increased the TV and PEF in COPD rats (Figure 4A and B). Similarly, BJF and aminophylline also could increase the 50% TV expiratory flow at week 20 (Figure 4C). In addition, lung injury scores, bronchiole wall thickness, small pulmonary vessels wall thickness, bronchiole stenosis, and alveolar diameter increased in the model rat, and this increase was clearly suppressed by the treatment of animals with BJF (Figure 5A–F). Moreover, BJF treatment also markedly increased the alveolar number in COPD rats (Figure 5G). These results suggested that BJF is an effective Chinese medicine for the treatment of COPD.

Many different studies have shown that comorbidities, such as cardiovascular, metabolic, muscular, and bone disorders, occur more frequently in patients with COPD than in smokers and never-smoked control subjects of similar age.[50,51] In this study, we also found that rats with COPD are at an increased risk of ventricular hypertrophy. Therefore, we examined the effects of BJF on ventricular hypertrophy, which is a common comorbidity of COPD. As shown in Figure 6, compared with the model rat, BJF significantly increased the myocardial sarcomere length and mitochondrial density of cardiocytes and reversed the RVHI at week 20. Furthermore, studies have demonstrated that hypertrophic stimuli, such as ET-1, TGF-β, VEGF, bFGF, and angiotensin II, can activate a range of hypertrophic signaling mediators and transcription factors, such as extracellular signal-regulated kinase 1/2 and nuclear factor-κB, and enhance myocardial angiogenesis.[53,54] In this work, we found that BJF clearly decreased the expression of VEGF, bFGF, TGF-β, and ET-1. Furthermore, the effects of BJF were higher than those of aminophylline (Figure 7).

These findings suggested that BJF treatment can effectively prevent COPD and ventricular hypertrophy, and these results are consistent with those obtained by the target–disease network.

Effect of BJF on inflammatory responses in COPD rats

In the systems pharmacology study, we found that numerous prediction targets of BJF are related to activation of the activator protein-1 family of transcription factors and

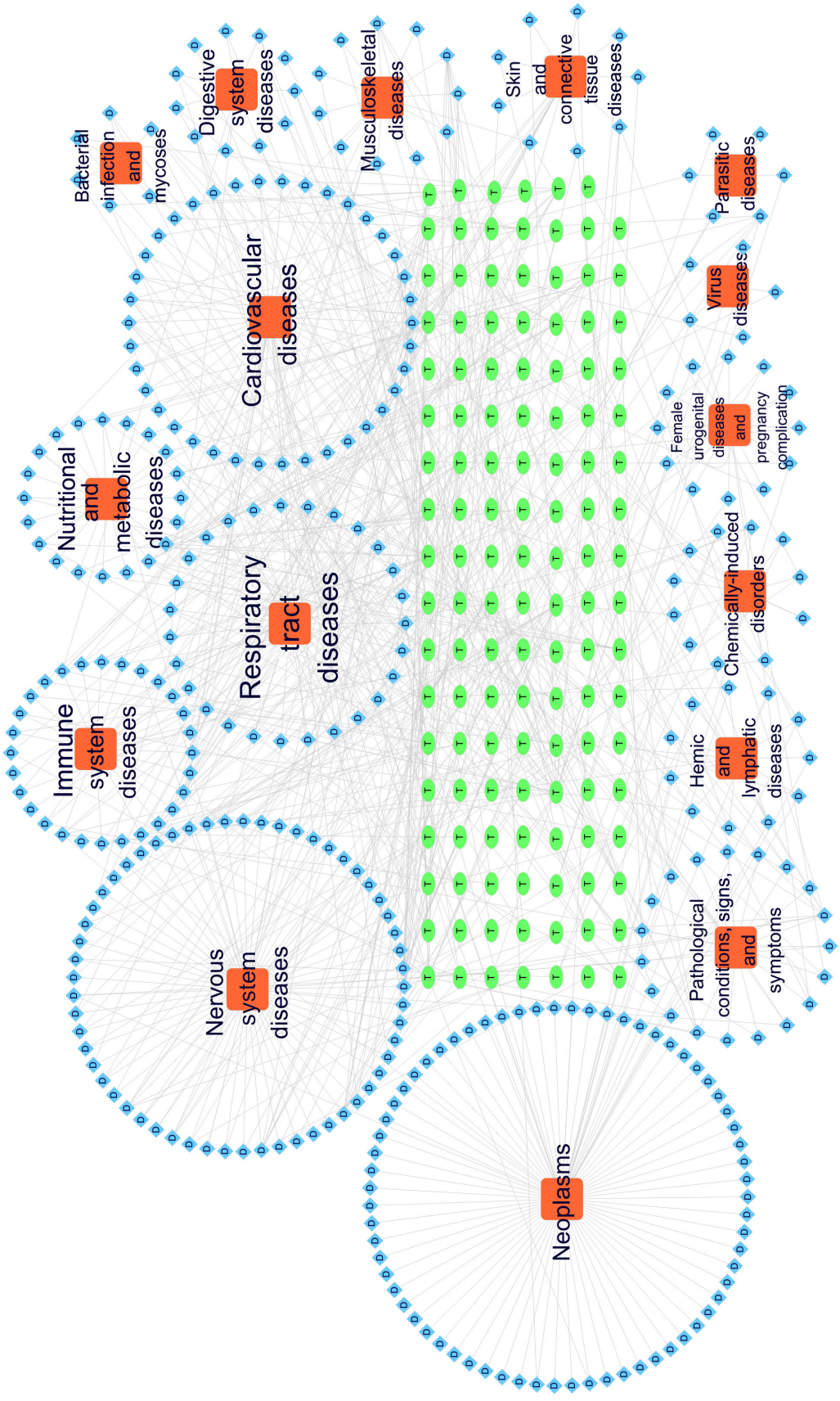

Figure 3 Target–disease network (T–D network).
Notes: In the T–D network, candidate targets were connected with related diseases. Target proteins (133, ellipse, green) are connected to 348 diseases (rhombus, blue), which are classified into 16 groups (square, orange).
Abbreviations: D, disease; T, target.

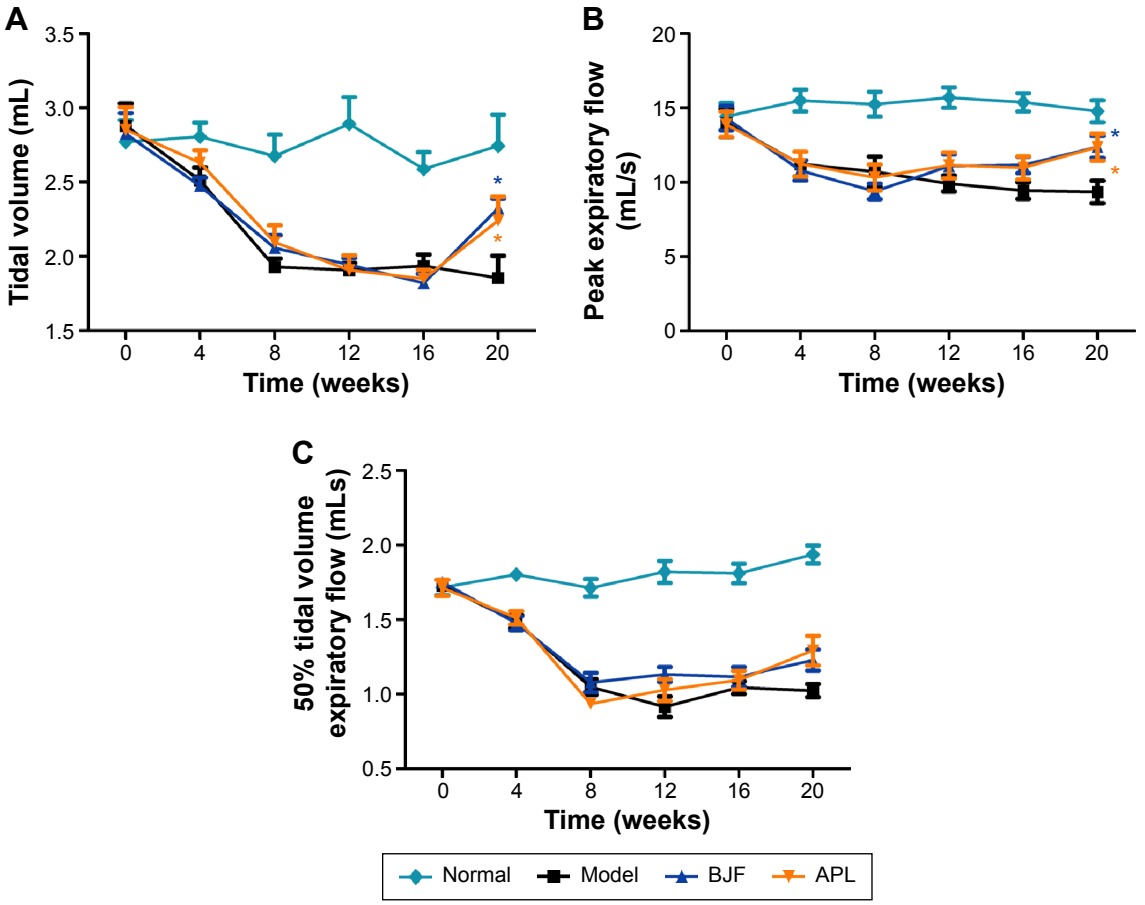

Figure 4 Effect of Bufei Jianpi formula (BJF) and aminophylline (APL) on pulmonary function of chronic obstructive pulmonary disease rats.
Notes: BJF (4.84 g/kg) and APL (2.3 mg/kg) were administered intragastrically once daily from weeks 9 to 20. Tidal volume (**A**), peak expiratory flow (**B**), and 50% tidal volume expiratory flow (**C**) were detected every 4th week from weeks 0 to 20. Values represent the mean ± standard error of mean. *$P<0.05$ vs model.

MAPK targets/nuclear events mediated by MAPK, which play important roles in inflammatory responses, such as inflammatory cytokines production. Many studies have shown that airway inflammation of COPD patients, both acute and chronic, is induced by cytokines, such as ILs (IL-1β, IL-4, IL-6, IL-10, and IL-13) and TNF-α, and other mediators, such as the cysteinyl leukotrienes and isoprostanes.[52] To verify this prediction, we examined the levels of inflammatory cytokines in the lung of COPD rats. As shown in Figure 8, levels of IL-6, IL-10, TNF-α, and soluble TNF-α receptor 2 increased after the cigarette smoke and bacterial infection exposures, and this increase was clearly suppressed by the treatment of animals with BJF. These results demonstrated that BJF achieves its anti-inflammatory activity by decreasing the levels of inflammatory cytokines in the lung, which also is consistent with the results obtained by target protein function analysis.

Effect of BJF on collagen degradation and protease–antiprotease imbalance

A protease–antiprotease imbalance leads to the breakdown of connective tissue components and is the critical mechanism in the pathogenesis of COPD. Furthermore, there is increasing interest in the role of MMPs in COPD.[55] Increased concentrations of MMP-2 and MMP-9 were observed in bronchoalveolar lavage fluid from COPD patients, and there is increased activity of MMP-9 and decreased activity of TIMP-1 in the lung parenchyma.[56,57] In COPD, abnormally high collagen remodeling also occurs within the lung tissue. In particular, the turnover rate of type I, III, and IV collagen is changed significantly, leading to excessive remodeling and accumulation of structural proteins.[58] In this work, the systems pharmacology study suggested that the potential targets were related to activation of MMPs. Therefore, we examined the effect of BJF on the expression of MMP-2, MMP-9, TIMP-1, and collagens I, III, and IV in lung tissues. As shown in Figure 9A, BJF treatment clearly decreased the levels of MMP-2 and MMP-9 and increased the level of TIMP-1. This alteration also was observed at the messenger RNA level (Figure 9B). As shown in Figure 10, collagens I, III, and IV were increased significantly by the cigarette smoke and bacterial infection exposures, and this increase was markedly suppressed by the treatment of animals with BJF.

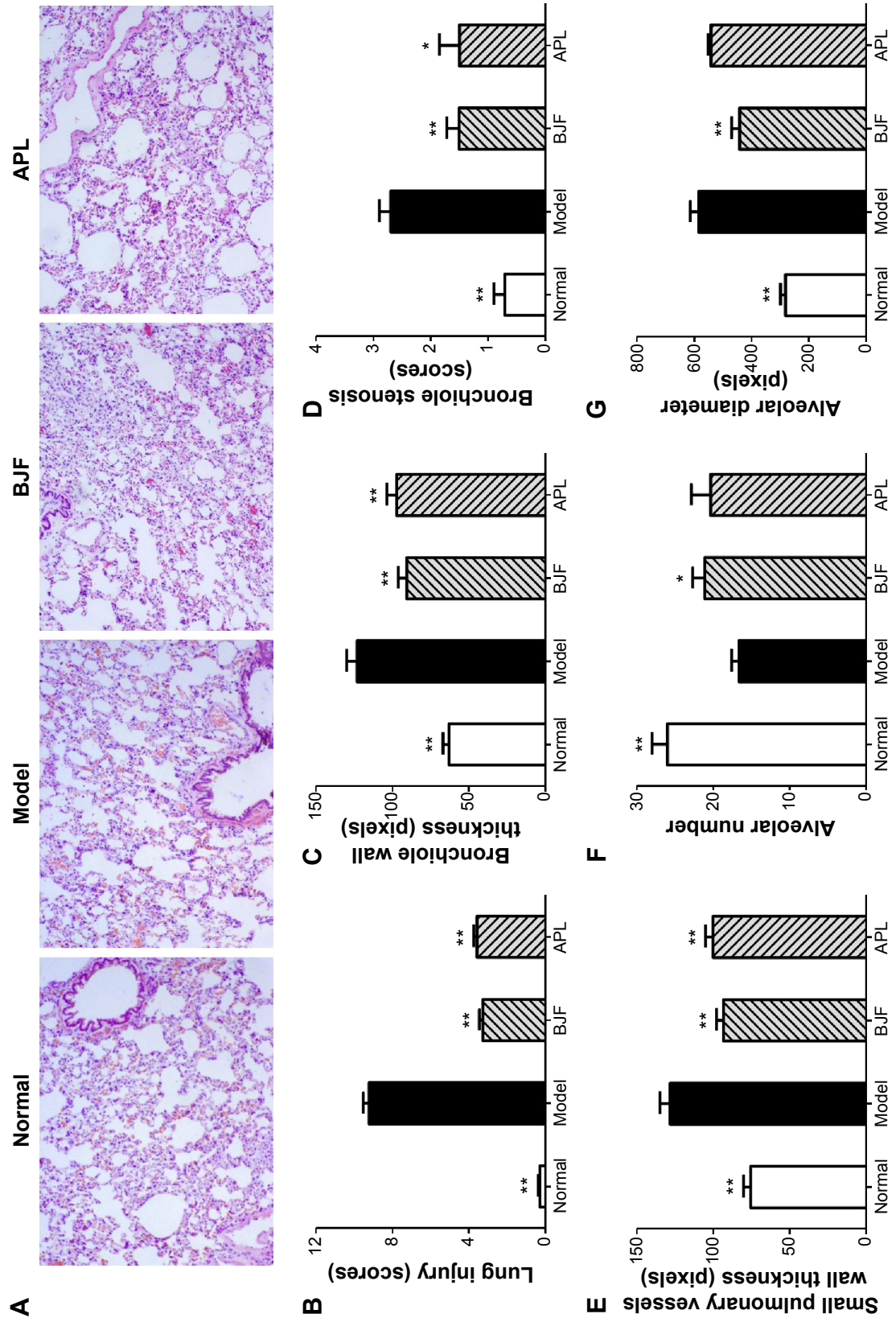

Figure 5 Effects of Bufei Jianpi formula (BJF) and aminophylline (APL) on histological changes in hematoxylin and eosin (H&E)-stained lung sections of chronic obstructive pulmonary disease (COPD) rats.
Notes: On week 20, the lung tissues of COPD rats were collected. Histological changes were detected using H&E staining (original magnification ×100) (**A**). The lung injury scores of all groups were summarized (**B**). Bronchial wall thickness (**C**), bronchiole stenosis (**D**), small pulmonary vessels wall thickness (**E**), alveolar number (**F**), and alveolar diameter (**G**) were evaluated. Values represent the mean ± standard error of mean. *$P<0.05$, **$P<0.01$ vs model.

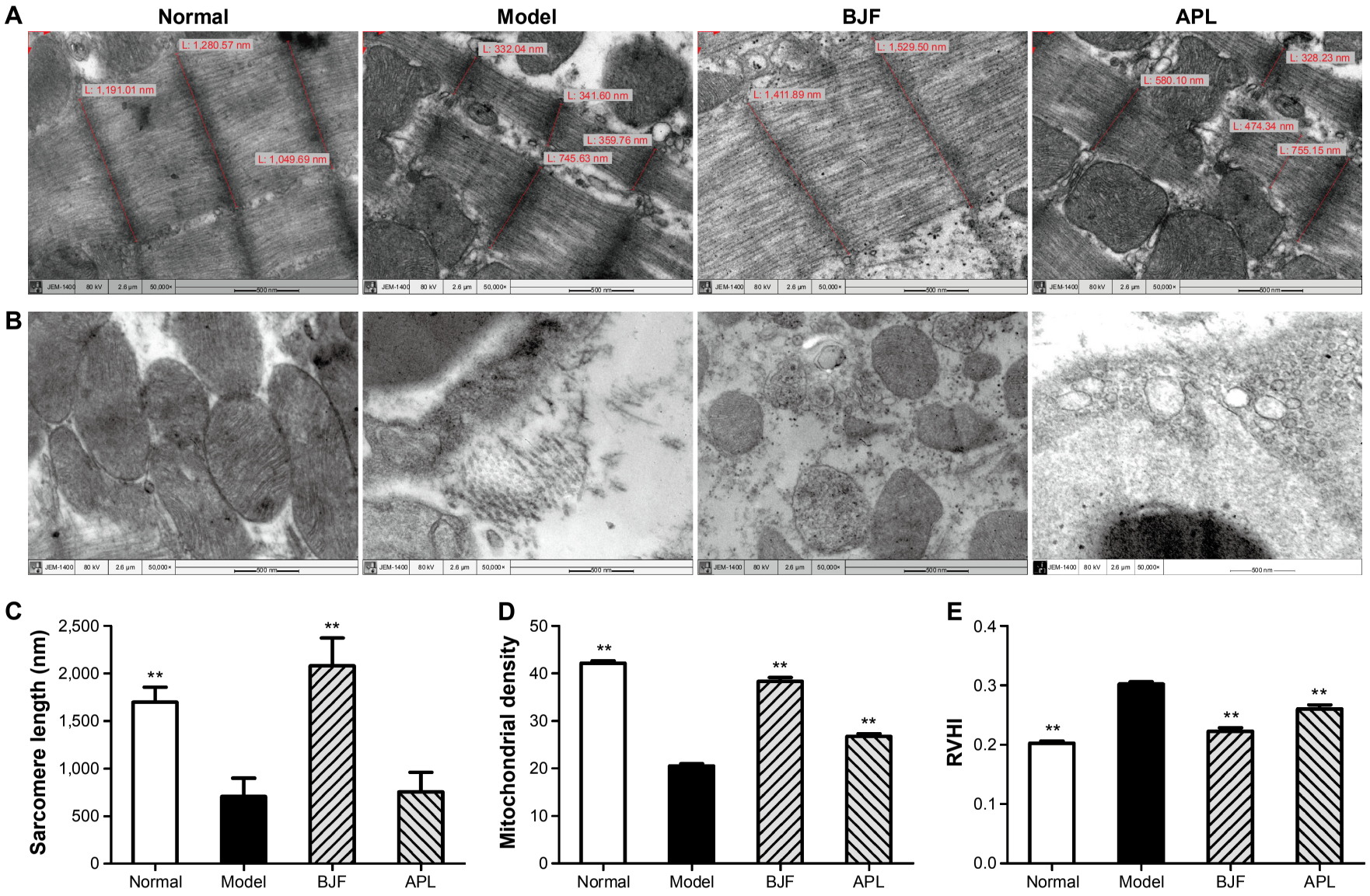

Figure 6 Effect of Bufei Jianpi formula (BJF) and aminophylline (APL) on changes in the myocardial ultrastructure and the right ventricular hypertrophy index (RVHI) of chronic obstructive pulmonary disease rats.
Notes: The muscular fibers (**A**) and mitochondria (**B**) of myocardial ultrastructure images were taken by transmission electron microscope (original magnification ×50,000). The sarcomere length (**C**), mitochondrial density (**D**), and RVHI (**E**) were evaluated. Values represent the mean ± standard error of mean. $^{**}P<0.01$ vs model.

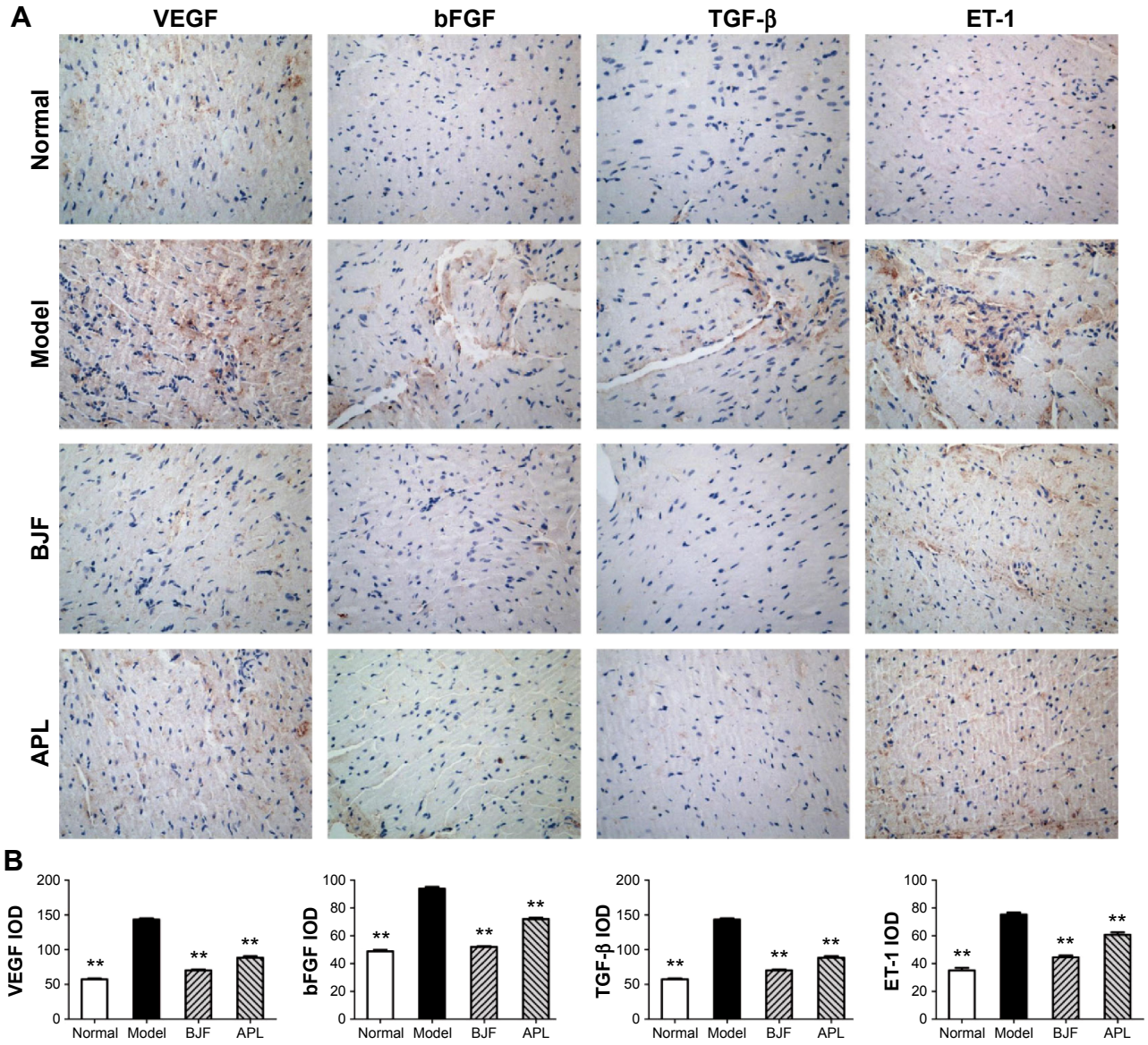

Figure 7 Effect of BJF and APL on the expression of VEGF, bFGF, TGF-β, and ET-1 around the right ventricle obtained from chronic obstructive pulmonary disease rats.
Notes: Immunohistochemical staining of the right ventricle sections for VEGF, bFGF, TGF-β, and ET-1 (original magnification ×200) (**A**). Quantitative analysis for the expression of VEGF, bFGF, TGF-β, and ET-1 in the right ventricle (**B**). Values represent the mean ± standard error of mean. $^{**}P<0.01$ vs model.
Abbreviations: VEGF, vascular endothelial growth factor; bFGF, basic fibroblast growth factor; TGF-β, transforming growth factor-β; ET-1, endothelin 1; BJF, Bufei Jianpi formula; APL, aminophylline; IOD, integral optical density.

These results suggested that BJF suppressed the cigarette smoke- and bacterial infection-induced collagen deposition and protease–antiprotease imbalance by inhibiting the expression of collagens I, III, and IV, MMP-2/-9, and increasing the expression of TIMP-1.

From these results, systems pharmacology under the systems biology framework has been used successfully to investigate the active compounds of BJF and their targets and understand the multiple uses and molecular mechanisms of BJF. Furthermore, we experimentally validated that BJF suppressed cigarette smoke- and bacterial infection-induced pulmonary inflammation, collagen deposition, protease–antiprotease imbalance, and hypertrophic factor production, suggesting this formula could be effective for the treatment of COPD and its comorbidity.

Conclusion

TCM, an important part of natural medicine, greatly improves the efficiency for the treatment of complex diseases, especially COPD. Even though TCM has accumulated much clinical experience and provided many effective applications, it always has been discredited as a mystery due to a lack of

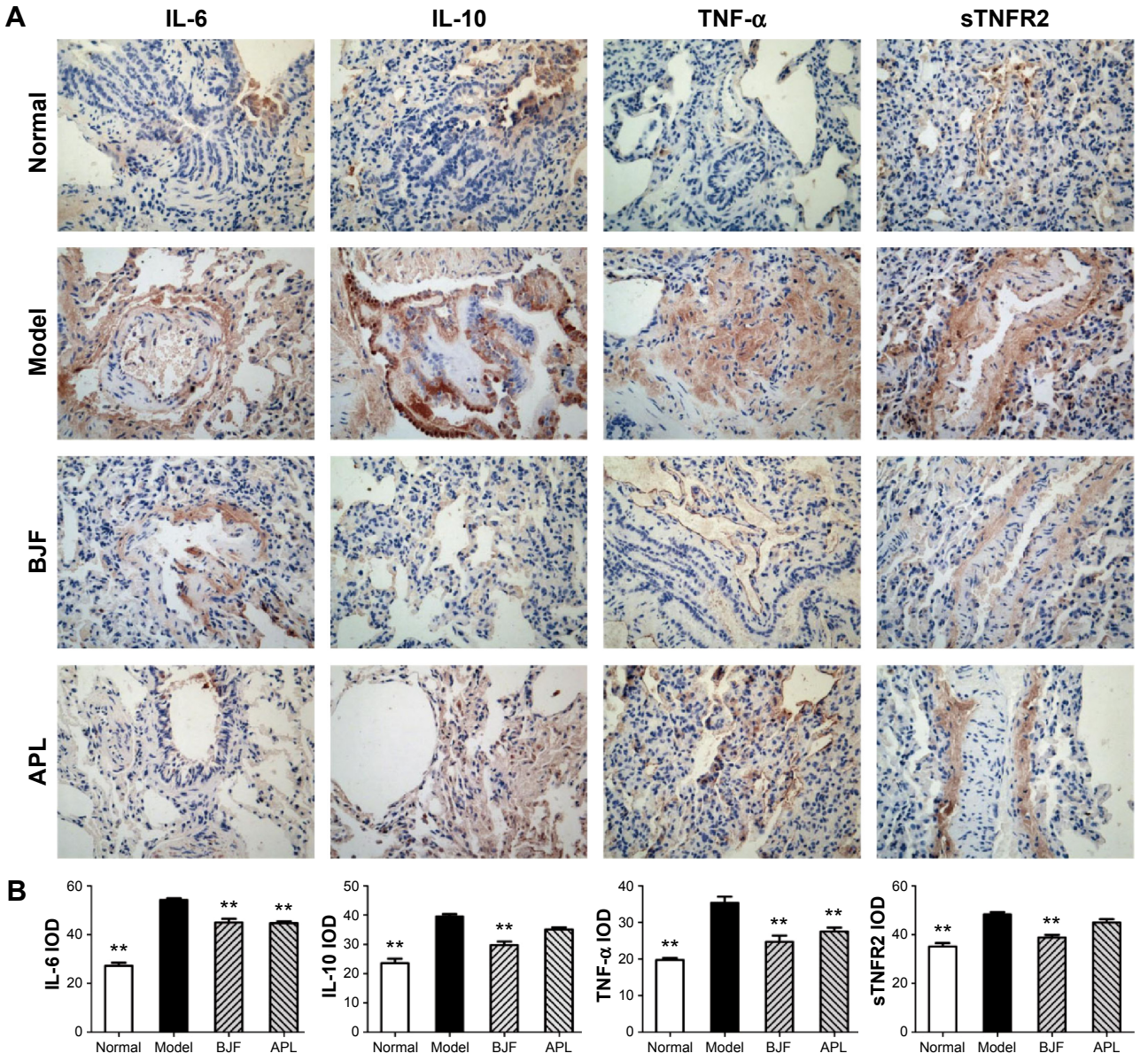

Figure 8 Effect of Bufei Jianpi formula (BJF) and aminophylline (APL) on the expression of interleukin (IL)-6, IL-10, tumor necrosis factor (TNF)-α, and soluble TNF-α receptor 2 (sTNFR2) in the lung obtained from chronic obstructive pulmonary disease (COPD) rats.

Notes: Immunohistochemical staining of lung sections for IL-6, IL-10, TNF-α, and sTNFR2 (original magnification ×200) (**A**). Quantitative analysis for the expression of IL-6, IL-10, TNF-α, and sTNFR2 in the lung of COPD rats (**B**). Values represent the mean ± standard error of mean. $^{**}P<0.01$ vs model.

Abbreviation: IOD, integral optical density.

systems methods for identifying the bioactive ingredients and their therapeutic targets. In this work, we proposed a systems pharmacology approach to dissect the molecular mechanisms of the action of BJF by systematically incorporating OB prediction, target proteins prediction, and the target-related disease network analysis. In addition, a rat model of cigarette smoke- and bacterial infection-induced COPD was applied to validate the effects and mechanism of BJF on COPD and its comorbidity. The main findings are as follows. 1) The candidate ingredients and their potential targets in the BJF prescriptions were identified, which provided insights into the synergetic effects of BJF and clues to clarify the mechanisms of BJF for the prevention of COPD and other diseases. 2) The target–disease network showed that BJF has efficiency not only for the treatment of COPD but also for other diseases, such as neoplasms, nervous system diseases, cardiovascular disease, and musculoskeletal diseases, suggesting that different diseases can be treated with the same formula. 3) The experimental study found that BJF ameliorated COPD and its comorbidity in vivo via mechanisms that are dependent on its effects on inflammatory cytokine production, MMP expression, collagen deposition,

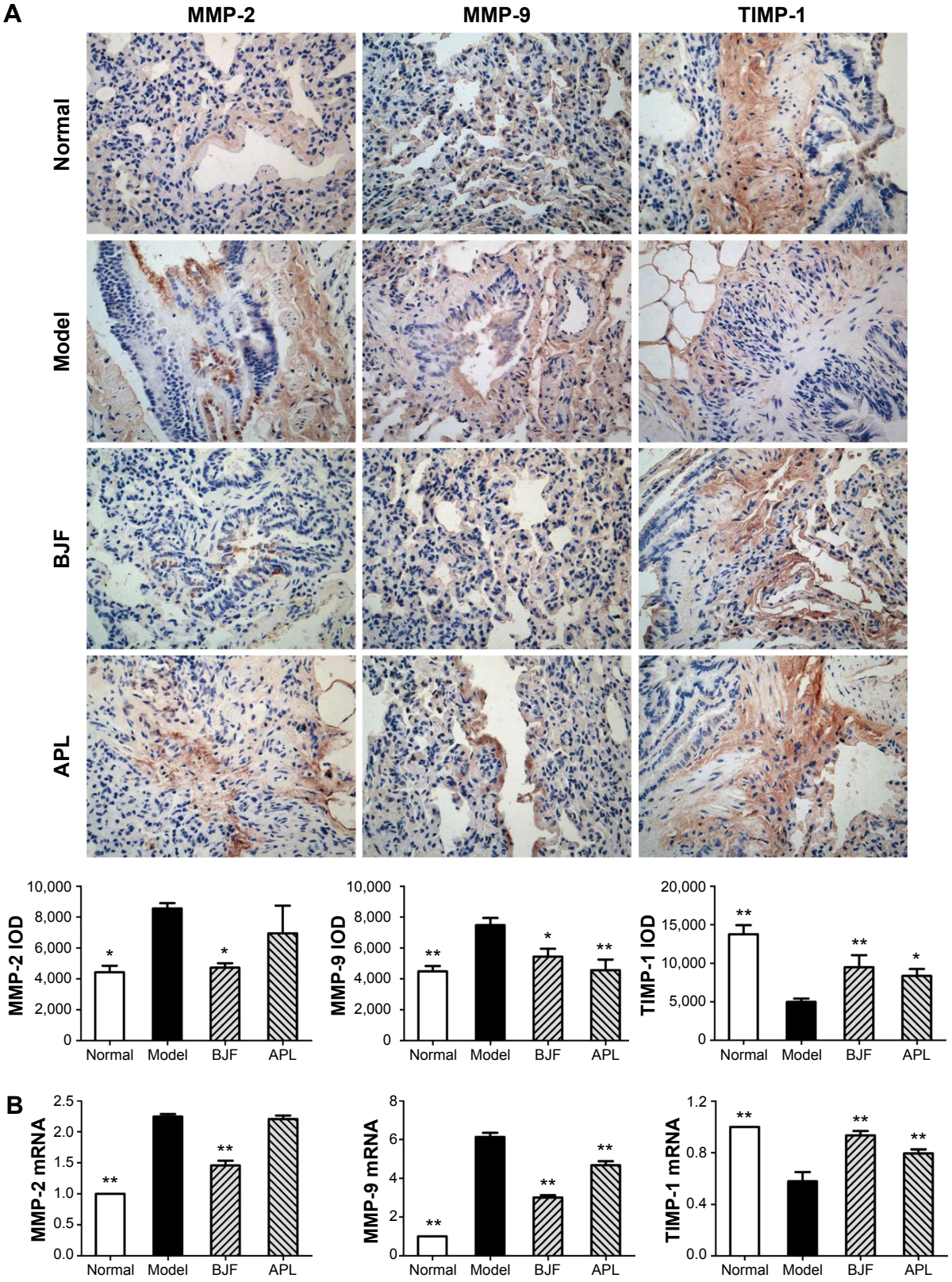

Figure 9 Effect of Bufei Jianpi formula (BJF) and aminophylline (APL) on the expression of matrix metalloproteinase (MMP)-2, MMP-9, and tissue inhibitor of MMP (TIMP)-1 in the lung obtained from chronic obstructive pulmonary disease (COPD) rats.

Notes: Immunohistochemical and quantitative analysis for the expression of MMP-2, MMP-9, and TIMP-1 in the lung of COPD rats (original magnification ×200) (**A**). The messenger RNA (mRNA) levels of MMP-2, MMP-9, and TIMP-1 were analyzed with reverse transcriptase-polymerase chain reaction (**B**). Data are presented as mean ± standard error of mean. *$P<0.05$, **$P<0.01$ vs model.

Abbreviation: IOD, integral optical density.

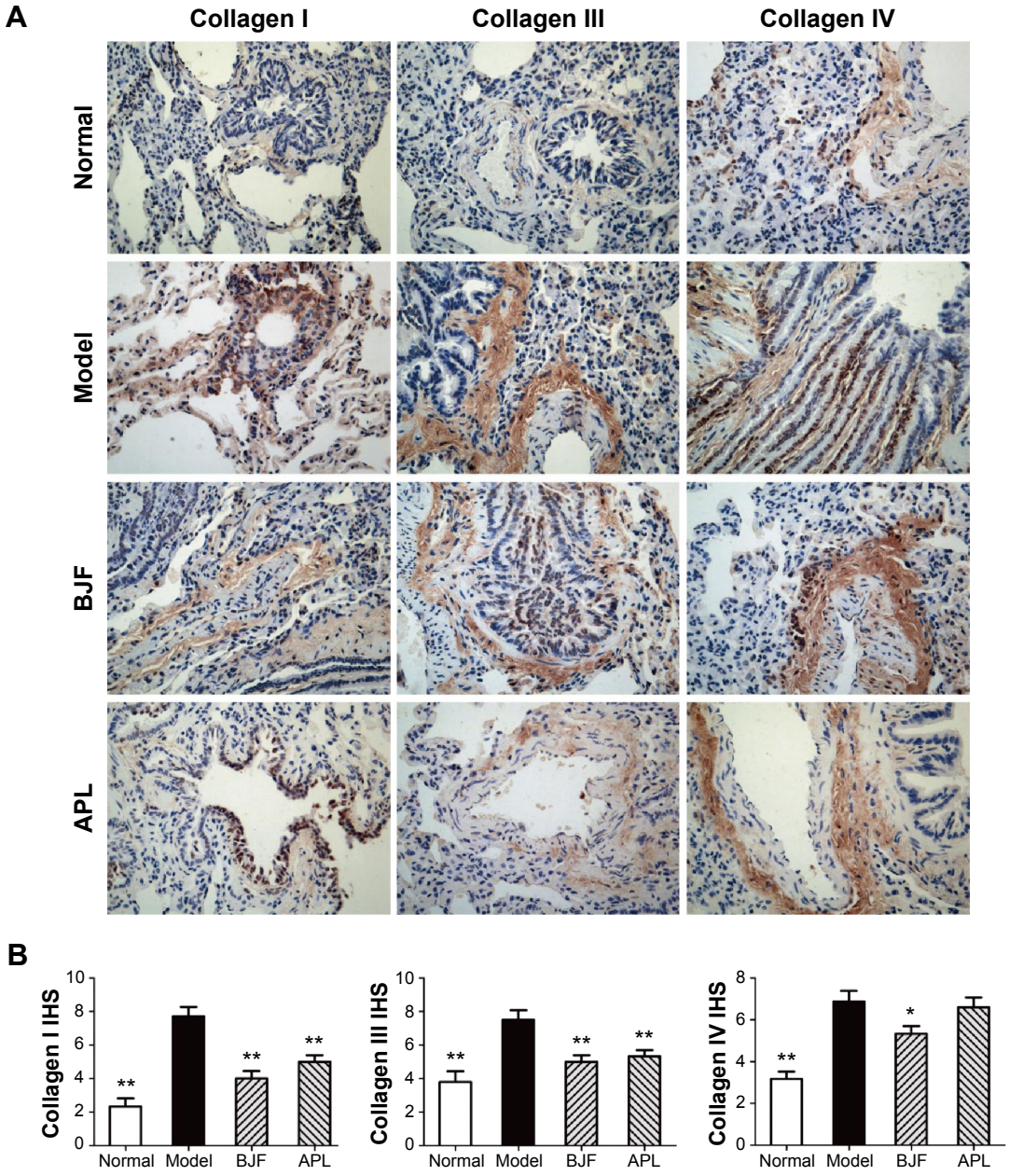

Figure 10 Effect of Bufei Jianpi formula (BJF) and aminophylline (APL) on the expression of collagens I, III, and IV in the lung obtained from chronic obstructive pulmonary disease (COPD) rats.

Notes: Immunohistochemical analysis for the expression of collagens I, III, and IV in the lung of COPD rats (original magnification ×200) (**A**). Quantitative analysis for the expression of collagens I, III, and IV in the lungs of COPD rats (**B**). Data are presented as mean ± standard error of mean. *$P<0.05$, **$P<0.01$ vs model.

Abbreviation: IHS, immunohistochemical score.

and other cytokine production, and these results were consistent with the predictions of the systems pharmacology studies. 4) The integrated systems pharmacology platform constructed in this work illuminated the effects and mechanisms of BJF on COPD and its comorbidity, which provides valuable insights to support the development of novel drugs.

In summary, systems pharmacology currently describes an innovative research field of study that incorporates experimental and computational approaches to explain both active ingredients and targets of TCM, which could help us to explore the complex TCM mechanism-of-action profiles and promote TCM modernization in the future study. The major limitation of this study is its direct demand for further experimental validation such as the proportion of every component, which will be resolved in the follow-up studies.

Acknowledgments

The research is supported by National Natural Science Fund of China (Influence and Long-Term Effects of Three

Tiao-Bu Fei-Shen Therapies in Rats with Chronic Obstructive Pulmonary Disease on Regulation of Multidimensional Molecular Network, 81130062).

Author contributions

JSL and YHW designed the outline of the study, and contributed toward data analysis and critically revising the paper. PZ performed experiments, conceived the study, wrote the draft and revised the manuscript. YGT and YL were involved in performing experiments, acquisition of data, and statistical analysis. CLZ contributed to the data analysis and interpretation. All authors contributed toward data analysis, drafting and critically revising the paper, gave final approval of the version to be published, and agree to be accountable for all aspects of the work.

Disclosure

The authors report no conflicts of interest in this work.

References

1. Murray CJ, Lopez AD. Measuring the global burden of disease. *N Engl J Med*. 2013;369:448–457.
2. Vestbo J, Hurd SS, Agusti AG, et al. Global strategy for the diagnosis, management, and prevention of chronic obstructive pulmonary disease: GOLD executive summary. *Am J Respir Crit Care Med*. 2013;187:347–365.
3. Wang G, Wang R, Strulovici-Barel Y, et al. Persistence of smoking-induced dysregulation of MiRNA expression in the small airway epithelium despite smoking cessation. *PloS One*. 2015;10:e0120824.
4. Park H, Shin JW, Park SG, Kim W. Microbial communities in the upper respiratory tract of patients with asthma and chronic obstructive pulmonary disease. *PloS One*. 2014;9:e109710.
5. Barnes PJ. Theophylline: new perspectives for an old drug. *Am J Respir Crit Care Med*. 2003;167:813–818.
6. Barnes PJ, Stockley RA. COPD: current therapeutic interventions and future approaches. *Eur Respir J*. 2005;25:1084–1106.
7. Alsaeedi A, Sin DD, McAlister FA. The effects of inhaled corticosteroids in chronic obstructive pulmonary disease: a systematic review of randomized placebo-controlled trials. *Am J Med*. 2002;113:59–65.
8. Barnes PJ, Ito K, Adcock IM. Corticosteroid resistance in chronic obstructive pulmonary disease: inactivation of histone deacetylase. *Lancet*. 2004;363:731–733.
9. Li SY, Li JS, Wang MH, et al. Effects of comprehensive therapy based on traditional Chinese medicine patterns in stable chronic obstructive pulmonary disease: a four-center, open-label, randomized, controlled study. *BMC Complement Altern Med*. 2012;12:197.
10. Zhao J, Jiang P, Zhang W. Molecular networks for the study of TCM pharmacology. *Brief Bioinform*. 2010;11:417–430.
11. Normile D. Asian medicine. The new face of traditional Chinese medicine. *Science*. 2003;299:188–190.
12. Hopkins AL. Network pharmacology. *Nat Biotechnol*. 2007;25:1110–1111.
13. Barabasi AL. Scale-free networks: a decade and beyond. *Science*. 2009;325:412–413.
14. Wang Z, Liu J, Yu Y, et al. Modular pharmacology: the next paradigm in drug discovery. *Expert Opin Drug Discov*. 2012;7:667–677.
15. Janga SC, Tzakos A. Structure and organization of drug-target networks: insights from genomic approaches for drug discovery. *Mol BioSyst*. 2009;5:1536–1548.
16. van der Greef J. Perspective: all systems go. *Nature*. 2011;480:S87.
17. Naseer S, Lone SH, Lone JA, Khuroo MA, Bhat KA. LC-MS guided isolation, quantification and antioxidant evaluation of bioactive principles from Epimedium elatum. *J Chromatogr B Analyt Technol Biomed Life Sci*. 2015;989:62–70.
18. Yan R, Yu S, Liu H, Xue Z, Yang B. An HPLC-DAD method for simultaneous quantitative determination of four active hydrophilic compounds in Magnoliae officinalis cortex. *J Chromatogr Sci*. 2015;53(4):598–602.
19. Liu Z, Jin Y, Shen P, Wang J, Shen Y. Separation and purification of verticine and verticinone from Bulbus Fritillariae Thunbergii by high-speed counter-current chromatography coupled with evaporative light scattering detection. *Talanta*. 2007;71(5):1873–1876.
20. Liu X, Cao P, Zhang C, et al. Screening and analyzing potential hepatotoxic compounds in the ethanol extract of Asteris Radix by HPLC/DAD/ESI-MS(n) technique. *J Pharm Biomed Anal*. 2012;67–68:51–62.
21. Nemeth K, Plumb GW, Berrin JG, et al. Deglycosylation by small intestinal epithelial cell beta-glucosidases is a critical step in the absorption and metabolism of dietary flavonoid glycosides in humans. *Eur J Nutr*. 2003;42:29–42.
22. van der Graaf PH, Benson N. Systems pharmacology: bridging systems biology and pharmacokinetics-pharmacodynamics (PKPD) in drug discovery and development. *Pharm Res*. 2011;28:1460–1464.
23. Xu X, Zhang W, Huang C, et al. A novel chemometric method for the prediction of human oral bioavailability. *Int J Mol Sci*. 2012;13:6964–6982.
24. Ma C, Wang L, Xie XQ. GPU accelerated chemical similarity calculation for compound library comparison. *J Chem Inf Model*. 2011;51:1521–1527.
25. Wang A, Xiao Z, Zhou L, Zhang J, Li X, He Q. The protective effect of atractylenolide I on systemic inflammation in the mouse model of sepsis created by cecal ligation and puncture. *Pharm Biol*. 2015:1–5.
26. Yao CM, Yang XW. Bioactivity-guided isolation of polyacetylenes with inhibitory activity against NO production in LPS-activated RAW264.7 macrophages from the rhizomes of atractylodes macrocephala. *J Ethnopharmacol*. 2014;151:791–799.
27. Chen KB, Chen HY, Chen KC. Treatment of cardiovascular disease by traditional Chinese medicine against pregnane X receptor. *Biomed Res Int*. 2014;2014:950191.
28. Pluchino LA, Liu AK, Wang HC. Reactive oxygen species-mediated breast cell carcinogenesis enhanced by multiple carcinogens and intervened by dietary ergosterol and mimosine. *Free Radic Biol Med*. 2015;80:12–26.
29. Manna K, Das U, Das D, et al. Naringin inhibits gamma radiation-induced oxidative DNA damage and inflammation, by modulating p53 and NF-kappaB signaling pathways in murine splenocytes. *Free Radic Res*. 2015;49:422–439.
30. Ciftci O, Ozcan C, Kamisli O, Cetin A, Basak N, Aytac B. Hesperidin, a citrus flavonoid, has the ameliorative effects against experimental autoimmune encephalomyelitis (EAE) in a C57BL/J6 mouse model. *Neurochem Res*. 2015;40:1111–1120.
31. Park JS, Park HY, Rho HS, Ahn S, Kim DH, Chang IS. Statistically designed enzymatic hydrolysis for optimized production of icariside II as a novel melanogenesis inhibitor. *J Microbiol Biotechnol*. 2008;18:110–117.
32. Li Y, Zhang X, Peng H, Li R, Deng X. Effects of anhydroicaritin and 2″-hydroxy-3″-en-anhydroicaritin on the proliferation and differentiation of MC3T3-E1 osteoblasts. *Nat Prod Commun*. 2012;7:1461–1464.
33. Gao XJ, Guo MY, Zhang ZC, et al. Bergenin plays an anti-inflammatory role via the modulation of MAPK and NF-kappaB signaling pathways in a mouse model of LPS-induced mastitis. *Inflammation*. 2014;38:1142–1150.
34. Yu H, Chen J, Xu X, et al. A systematic prediction of multiple drug-target interactions from chemical, genomic, and pharmacological data. *PloS One*. 2012;7:e37608.
35. Smoot ME, Ono K, Ruscheinski J, Wang PL, Ideker T. Cytoscape 2.8: new features for data integration and network visualization. *Bioinformatics*. 2011;27:431–432.

36. Assenov Y, Ramirez F, Schelhorn SE, Lengauer T, Albrecht M. Computing topological parameters of biological networks. *Bioinformatics*. 2008;24:282–284.
37. Li Y, Li SY, Li JS, et al. A rat model for stable chronic obstructive pulmonary disease induced by cigarette smoke inhalation and repetitive bacterial infection. *Biol Pharm Bull*. 2012;35:1752–1760.
38. Hnizdo E. Lung function loss associated with occupational dust exposure in metal smelting. *Am J Respir Crit Care Med*. 2010;181:1162–1163.
39. Veber DF, Johnson SR, Cheng HY, Smith BR, Ward KW, Kopple KD. Molecular properties that influence the oral bioavailability of drug candidates. *J Med Chem*. 2002;45:2615–2623.
40. Lv YC, Yang J, Yao F, et al. Diosgenin inhibits atherosclerosis via suppressing the MiR-19b-induced downregulation of ATP-binding cassette transporter A1. *Atherosclerosis*. 2015;240:80–89.
41. Morwood CJ, Lappas M. The citrus flavone nobiletin reduces pro-inflammatory and pro-labour mediators in fetal membranes and myometrium: implications for preterm birth. *PloS One*. 2014;9:e108390.
42. Chen C, Zhou J, Ji C. Quercetin: a potential drug to reverse multidrug resistance. *Life Sci*. 2010;87:333–338.
43. Lin Y, Shi R, Wang X, Shen HM. Luteolin, a flavonoid with potential for cancer prevention and therapy. *Curr Cancer Drug Targets*. 2008;8:634–646.
44. Cho JH, Jeon YJ, Park SM, et al. Multifunctional effects of honokiol as an anti-inflammatory and anti-cancer drug in human oral squamous cancer cells and xenograft. *Biomaterials*. 2015;53:274–284.
45. Suleyman H, Demircan B, Karagoz Y. Anti-inflammatory and side effects of cyclooxygenase inhibitors. *Pharmacol Rep*. 2007;59:247–258.
46. Ndisang JF. Cross-talk between heme oxygenase and peroxisome proliferator-activated receptors in the regulation of physiological functions. *Front Biosci (Landmark Ed)*. 2014;19:916–935.
47. Bindea G, Mlecnik B, Hackl H, et al. ClueGO: a Cytoscape plug-in to decipher functionally grouped gene ontology and pathway annotation networks. *Bioinformatics*. 2009;25:1091–1093.
48. Banerjee A, Koziol-White C, Panettieri R Jr. p38 MAPK inhibitors, IKK2 inhibitors, and TNFalpha inhibitors in COPD. *Curr Opin Pharmacol*. 2012;12:287–292.
49. Rahman I, MacNee W. Antioxidant pharmacological therapies for COPD. *Curr Opin Pharmacol*. 2012;12:256–265.
50. Park H, Shin JW, Park SG, Kim W. Microbial communities in the upper respiratory tract of patients with asthma and chronic obstructive pulmonary disease. *PloS One*. 2014;9:e109710.
51. Yoshihara D, Kurahashi H, Morita M, et al. PPAR-gamma agonist ameliorates kidney and liver disease in an orthologous rat model of human autosomal recessive polycystic kidney disease. *Am J Physiol Renal Physiol*. 2011;300:F465–F474.
52. Mohapatra SK, Guri AJ, Climent M, et al. Immunoregulatory actions of epithelial cell PPAR gamma at the colonic mucosa of mice with experimental inflammatory bowel disease. *PloS One*. 2010;5:e10215.
53. Roth M, Black JL. Transcription factors in asthma: are transcription factors a new target for asthma therapy? *Curr Drug Targets*. 2006;7:589–595.
54. Feary JR, Rodrigues LC, Smith CJ, Hubbard RB, Gibson JE. Prevalence of major comorbidities in subjects with COPD and incidence of myocardial infarction and stroke: a comprehensive analysis using data from primary care. *Thorax*. 2010;65:956–962.
55. Cavailles A, Brinchault-Rabin G, Dixmier A, et al. Comorbidities of COPD. *Eur Respir Rev*. 2013;22:454–475.
56. Barnes PJ. Cellular and molecular mechanisms of chronic obstructive pulmonary disease. *Clin Chest Med*. 2014;35:71–86.
57. Laskowski A, Woodman OL, Cao AH, et al. Antioxidant actions contribute to the antihypertrophic effects of atrial natriuretic peptide in neonatal rat cardiomyocytes. *Cardiovasc Res*. 2006;72:112–123.
58. Tham YK, Bernardo BC, Ooi JY, Weeks KL, McMullen JR. Pathophysiology of cardiac hypertrophy and heart failure: signaling pathways and novel therapeutic targets. *Arch Toxicol*. 2015;89:1401–1438.
59. Atkinson JJ, Senior RM. Matrix metalloproteinase-9 in lung remodeling. *Am J Respir Cell Mol Biol*. 2003;28:12–24.
60. Culpitt SV, Maziak W, Loukidis S, et al. Effect of high dose inhaled steroid on cells, cytokines, and proteases in induced sputum in chronic obstructive pulmonary disease. *Am J Respir Crit Care Med*. 1999;160:1635–1639.
61. Finlay GA, O'Driscoll LR, Russell KJ, et al. Matrix metalloproteinase expression and production by alveolar macrophages in emphysema. *Am J Respir Crit Care Med*. 1997;156:240–247.
62. Leeming DJ, Sand JM, Nielsen MJ, et al. Serological investigation of the collagen degradation profile of patients with chronic obstructive pulmonary disease or idiopathic pulmonary fibrosis. *Biomarker Insights*. 2012;7:119–126.